GEORGIA INSTITUTE OF TECHNOLOGY
OFFICE OF CONTRACT ADMINISTRATION
SPONSORED PROJECT INITIATION

Date: February 20, 1980

Project Title: Soil Radar Response Study

Project No: A-2590

Project Director: Dr. W. J. Steinway

Sponsor: NASA/John F. Kennedy Space Center; Kennedy Space Center, FL 32899

Agreement Period: From 2/15/80 Until 8/14/80 (Contract Term)

Type Agreement: Contract No. NAS10-9757 (Fixed-Price)

Amount: $9,985

Reports Required: Initial Study Plan; Monthly Progress Reports; Final Report

Sponsor Contact Person (s):

Technical Matters

NASA Technical Representative

Mr. John Kassak
NASA/John F. Kennedy Space Center
Kennedy Space Center, FL 32899

Contractual Matters
(thru OCA)

William R. Harris
Contracting Officer
Procurement Office
NASA/John F. Kennedy Space Center
Kennedy Space Center, FL 32899

Defense Priority Rating: None

Assigned to: RAIL/RAD (School/Laboratory)

COPIES TO:

Project Director
Division Chief (EES)
School/Laboratory Director
Dean/Director–EES
Accounting Office
Procurement Office
Security Coordinator (OCA)
Reports Coordinator (OCA)
Library, Technical Reports Section
EES Information Office
EES Reports & Procedures
Project File (OCA)
Project Code (GTRI)
Other

GEORGIA INSTITUTE OF TECHNOLOGY
OFFICE OF CONTRACT ADMINISTRATION

SPONSORED PROJECT TERMINATION

Date: 12/5/80

Project Title: Soil Radar Response Study

Project No: A-2590

Project Director: Dr W J Steinway

Sponsor: NASA/John F Kennedy Space Center; Kennedy Space Center, FL 32899

Effective Termination Date: 10/14/80 (Fixed-Price)

Clearance of Accounting Charges: —

Grant/Contract Closeout Actions Remaining:

- X Final Invoice ~~and Closing Documents~~
- _ Final Fiscal Report
- X Final Report of Inventions
- X Govt. Property Inventory & Related Certificate
- _ Classified Material Certificate
- _ Other _____

Assigned to: RAIL/RAD (School/Laboratory)

COPIES TO:

- Project Director
- Division Chief (EES)
- School/Laboratory Director
- Dean/Director–EES
- Accounting Office
- Procurement Office
- Security Coordinator (OCA)
- ✓ Reports Coordinator (OCA)
- Library, Technical Reports Section
- EES Information Office
- Project File (OCA)
- Project Code (GTRI)
- Other _____

CA–4 (1/79)

A-2590

Georgia Institute of Technology
ENGINEERING EXPERIMENT STATION
ATLANTA, GEORGIA 30332

April 3, 1980

Mr. John Kassak
NASA/John F. Keendy Space Center
Kennedy Space Center, Florida 32899

Subject: Initial Study Plan for Contract No. NAS10-9757, Georgia Tech Project No. A-2590

Dear Mr. Kassak:

Enclosed is the initial study plan.

The proposed program comprises three primary tasks to be conducted according to the six month schedule as shown. A draft of the final technical report will be submitted at the end of the program.

Task 1 - Investigation of Modern Signal Analysis Techniques

Drawing from experience both in the past and from current on-going analysis efforts involving sub-surface radars and from literature, applicable modern signal analysis techniques will be singled out for application to sub-surface radar data. Particular attention will be paid to those techniques that provide improved resolution of sub-surface targets (i.e., pipes, rocks, soil interfaces, etc.), or provide enhancements of the data (i.e., eliminate reflections, etc.)

Task 2 - Data Editing, Digitizing, and Formatting

The digitizing and formatting of a sponsor supplied analog tape containing sub-surface radar data will be the initial part of this task. Data editing will then be used to select portions of the radar data to which a selected set of analysis techniques (from Task 1) will be applied. GIT/EES has available analog-to-digital conversion facilities, as well as several large digital computer facilities to perform this data editing task.

Task 3 - Application of Selected Techniques

The specific set of techniques chosen from Task 1 will be applied to the data selected under Task 2 in order to demonstrate that the study goals have been

achieved. The results will indicate how well the analysis techniques resolve targets, detect soil interfaces, indicate soil mixes, detect voids, etc., up to a depth of two meters.

Respectfully submitted,

William J. Steinway
Project Director

Approved:

J. D. Echard, Chief
Radar Applications Division

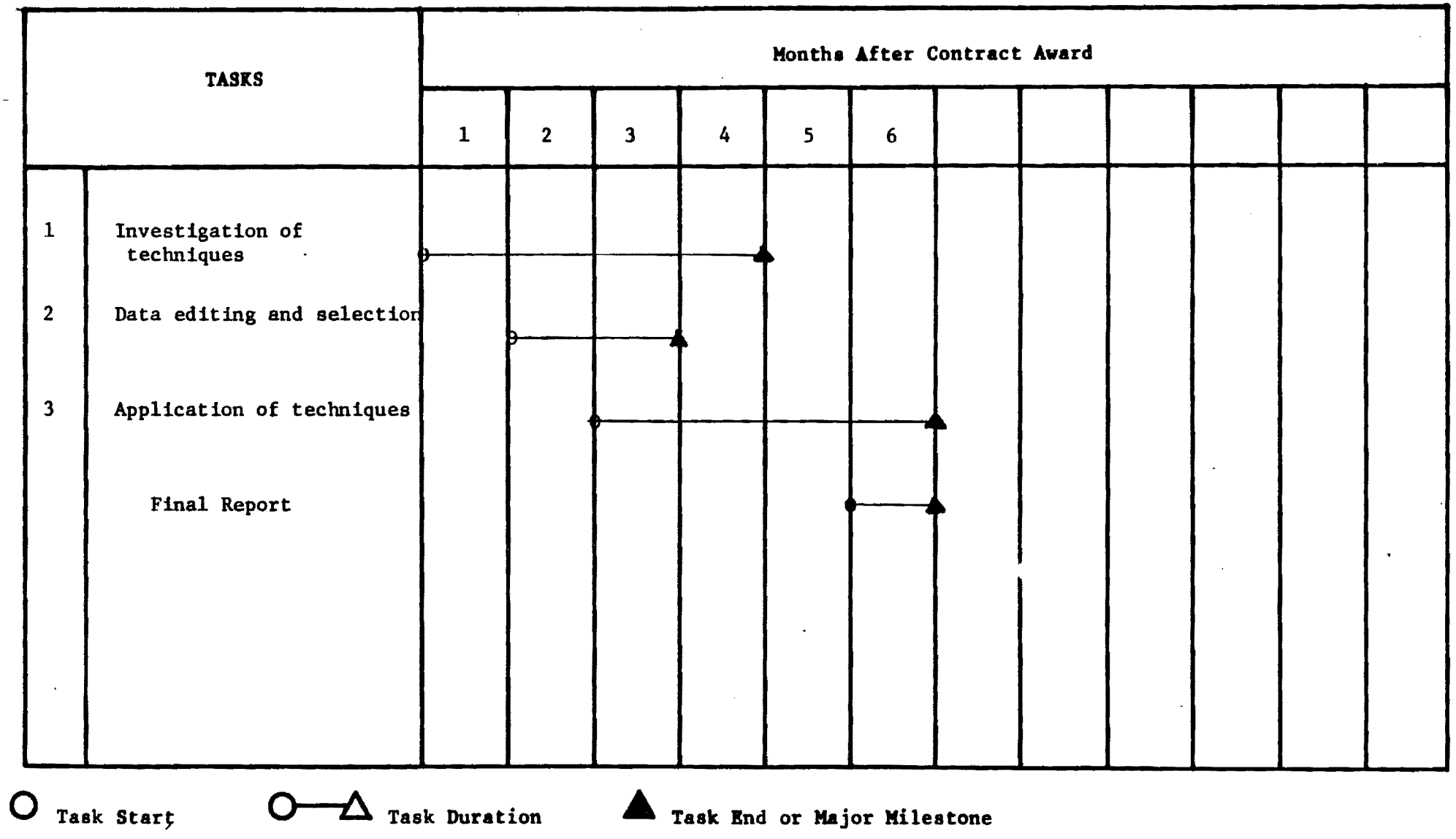
TASKS
Months After Contract Award
1
2
3
4
5
6
1 Investigation of techniques
2 Data editing and selection
3 Application of techniques
Final Report
Task Start
Task Duration
Task End or Major Milestone

A-2590

Georgia Institute of Technology
ENGINEERING EXPERIMENT STATION
ATLANTA, GEORGIA 30332

April 4, 1980

Mr. John Kassak
NASA/John F. Keendy Space Center
Kennedy Space Center, Florida 32899

Subject: Monthly Progress Report for Contract No. NAS10-9757, Georgia Tech Project No. A-2590, covering the period February 15, 1980 through February 29, 1980

Dear Mr. Kassak:

During the period from February 15, 1980 through February 29, 1980, the only activity was a series of phone conversations between the sponsor and Georgia Institute of Technology pertaining to the work. A meeting was scheduled during March at John F. Kennedy Space Center.

Respectfully submitted,

William J. Steinway
Project Director

Approved:

J. D. Echard, Chief
Radar Applications Division

A-2590

Georgia Institute of Technology
ENGINEERING EXPERIMENT STATION
ATLANTA, GEORGIA 30332

June 2, 1980

Mr. John Kassak
NASA/John G. Kennedy Space Center
Kennedy Space Center, Florida 32899

Subject: Monthly Progress Report for Contract No. NASA10-9757, Georgia Tech Project No. A-2590, covering the period March 1, 1980 through March 31, 1980

Dear Mr. Kassak:

During the period from March 1, 1980 to March 31, 1980 the investigation of modern signal analysis techniques was initiated. Both time and frequency methods are being considered.

In the time domain: full and half-wave rectification, cross-over triggering, signal shape matching (pattern recognition) and time correlation. In the frequency domain: Fast Fourier Transform and Maximum Entropy Methods followed by pattern recognition.

Respecfully submitted,

William J. Steinway
Project Director

Approved:

J. D. Echard, Chief
Radar Applications Division

A-2590

Georgia Institute of Technology
ENGINEERING EXPERIMENT STATION
ATLANTA, GEORGIA 30332

June 3, 1980

Mr. John Kassak
NASA/John F. Kennedy Space Center
Kennedy Space Center, Florida 32899

Subject: Monthly Progress Report for Contract No. NASA10-9757, Georgia Tech Project No. A-2590, covering the period May 1, 1980 through May 31, 1980

Dear Mr. Kassak:

During the period from May 1, 1980 to May 31, 1980 the investigation of modern signal analysis techniques is continuing. In addition the data tape supplied by NASA has been digitized. Several short sections of data have been selected for preliminary processing.

Respectfully submitted,

William J. Steinway
Project Director

Approved:

J. D. Echard, Chief
Radar Applications Division

A-2592

Georgia Institute of Technology
ENGINEERING EXPERIMENT STATION
ATLANTA, GEORGIA 30332

July 1, 1980

Mr. John Kassak
NASA/John F. Kennedy Space Center
Kennedy Space Center, Florida 32899

Subject: Monthly Progress Report, Contract No. NAS10-9757, covering the period June 1, 1980 through June 30, 1980

Dear Mr. Kassak:

During the period from June 1, 1980 through June 30, 1980, the investigation of modern signal analysis techniques was completed. A description of the techniques considered and those singled out for application to the sub-surface radar data are being prepared. Task 1 will thus be complete.

Preliminary application of several techniques to the digitized data has pointed out errors that occurred during the digitizing process. The NASA supplied tape is being re-digitized and the processing techniques applied.

Respectfully submitted,

William J. Steinway
Project Director

Approved:

J. D. Echard, Chief
Radar Applications Division

WJS/dw

A-2590

Georgia Institute of Technology
ENGINEERING EXPERIMENT STATION
ATLANTA, GEORGIA 30332

August 11, 1980

Mr. John Kassak
NASA/John F. Kennedy Space Center
Kennedy Space Center, Florida 32899

Subject: Monthly Progress Report, Contract No. NAS10-9757, covering the period July 1, 1980 through July 31, 1980.

Dear Mr. Kassak:

During the period from July 1, 1980 through July 31, 1980, the task of theoretical modeling of the radar signal return from sub-surface soil layers was initiated. This was in anticipation of the extension being granted. An example of the initial computer simulation results are given in the attached figure. The sequence of plots shows the effect of increasing layer depth on signal returns. This type of simulation will help in determining the resolution of the transmitted waveform.

Respectfully submitted,

William J. Steinway
Project Director

APPROVED:

J. D. Echard, Chief
Radar Applications Division

Enclosure
WJS/dw

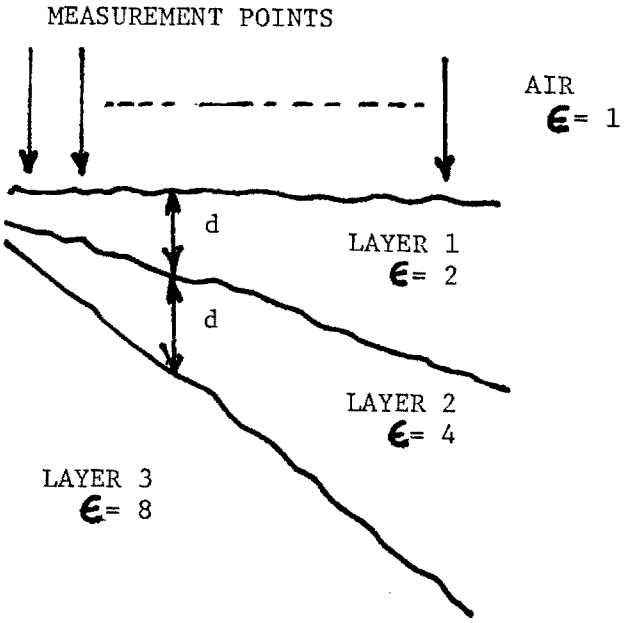

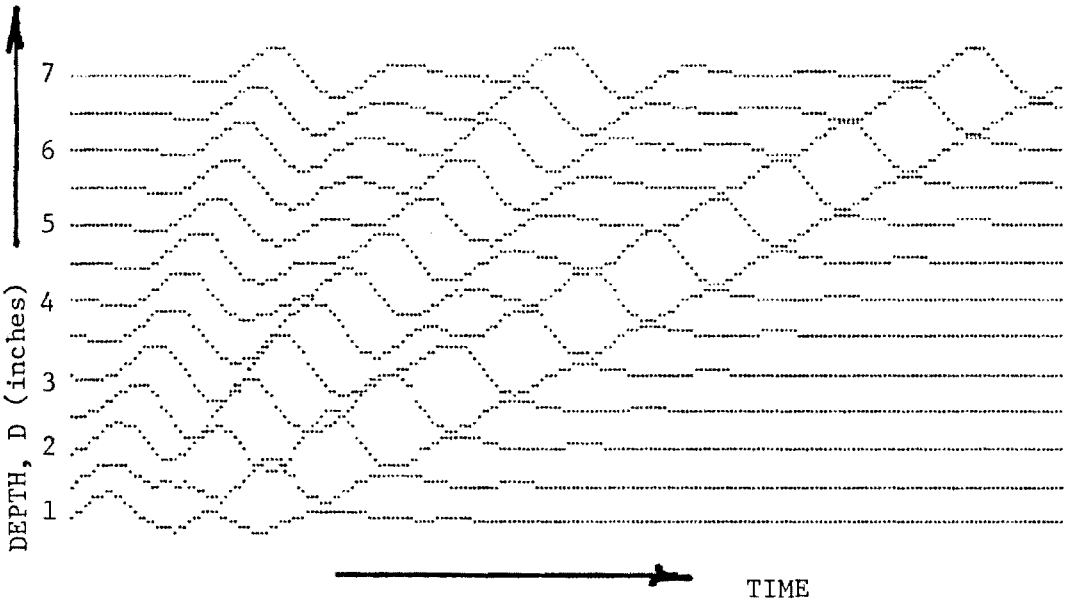

SIMULATED MEASUREMENTS

A-2590

Georgia Institute of Technology
ENGINEERING EXPERIMENT STATION
ATLANTA, GEORGIA 30332

September 20, 1980

Mr. John Kassak
NASA/John F. Kennedy Space Center
Kennedy Space Center, Florida 32899

Subject: Monthly Progress Report, Contract No. NAS10-9757, covering the period August 1, 1980 through August 31, 1980

Dear Mr. Kassak:

During the period from August 1, 1980 through August 31, 1980, the task of theoretical modeling of the radar signal return from sub-surface soil layers was completed. The errors that occured during the digitizing process were traced to hardware, and the problem corrected. An excellent quality digitized data tape has been generated. Processing techniques are now being applied to both real data and simulation data for verification.

Respectfully submitted,

William J. Steinway
Project Director

APPROVED:

J. D. Echard, Chief
Radar Applications Division

WJS/ss

A-2590

Georgia Institute of Technology
ENGINEERING EXPERIMENT STATION
ATLANTA, GEORGIA 30332

October 29, 1980

Mr. John Kassak
NASA/John F. Kennedy Space Center
Kennedy Space Center, Florida 32899

Subject: Monthly Progress Report, Contract No. NAS10-9757, covering the period September 1, 1980 through September 30, 1980

Dear Mr. Kassak:

During the period from September 1, 1980 through September 30, 1980, processing techniques were applied to the digitized data. The final report is in the preparation process. There will be approximately a one month delay in the delivery of the final report due to approval/reproduction cycle.

Respectfully submitted,

William J. Steinway
Project Director

APPROVED:

J. D. Echard, Chief
Radar Applications Division

WJS/ss

FINAL TECHNICAL REPORT

SOIL RESPONSE RADAR STUDY

Prepared for:

John F. Kennedy Space Center, NASA
Kennedy Space Center, Florida 32899

by

William J. Steinway
Jim D. Echard

Georgia Institute of Technology
Engineering Experiment Station
Atlanta, Georgia 30332

November 1980

TABLE OF CONTENTS

LIST OF FIGURES

1.0 INTRODUCTION

The following report describes the work done under contract number NAS10-9757, Georgia Institute of Technology/Engineering Experiment Station Project Number A-2590.

The purpose of this study is to enhance radar returns from soil layers by developing a method to eliminate superfluous multiple reflections, to determine soil layers which are obscured by the excitation pulse width, and to develop an analysis to calculate the theoretical resolution of the system. The objective is to identify applicable signal processing techniques which can be incorporated into the signal chain.

There is at present a technique, known as subsurface interface radar (SIR) sounding, wherein the subsurface features of soils can be mapped using a radar antenna in close proximity to the ground surface. In this technique, the antenna is enclosed in a box that can be dragged over the ground either behind a vehicle or manually.

The antenna is shock excited by a condenser discharge and oscillates at the natural frequency of vibration. Inasmuch as the ground is coupled into the antenna circuit, variations in the ground are coupled into the antenna circuit; also, variations in both the ground resistance and capacitance will affect the value of the oscillatory frequency. The oscillations are damped by the resistance of the circuit and die out after a few half cycles. The radar signal penetrates the ground, is reflected by a subsurface discontinuity, and the return signal is received and recorded.

If one single discrete subsurface discontinuity is assumed, then as many reflected signals will be received as there are outgoing half cycles in the signal (within the limits of the receiver sensitivity threshold). These multiple received reflected signals from a single subsurface discontinuity make for confusion and uncertainty in interpretation. In addition, the pulse width and multiple reflections obscure reflections which are immediately behind and within the pulse width.

Four tasks were undertaken during the study period: Investigation of Signal Analysis Techniques, Data Editing and Digitizing, Application of Processing Techniques, and Theoretical Modelling.

During the study it was found that the Theoretical Modelling provided the most insight into the interpretation and representation of signal returns. For the 'soil layer' classification problem, the resolution and accuracy of measurements were found to be most effected by antenna beamwidth and pulse resolution (bandwidth). Simple processing techniques were found to be most useful in realizing or displaying the full resolution capability for a given system. These simple methods could provide enough improvement in data display that actually improving the resolution via simple processing techniques by complicated signal processing techniques may be unnecessary. It was found that for most of the data supplied by NASA, that a realization of existing resolution via simple processing techniques significantly increases the system performance and data interpretation. Results of the signal processing techniques are most clearly illustrated on simulated data where the effects can be readily separated and identified. The overall effects upon actual measurement data (NASA supplied) are illustrated.

The next section of this report summarizes the Signal Processing techniques. Following that, the Theoretical Modelling, the Digitizing and Editing of Data and the Application of Processing Techniques are considered. This organization of the tasks appears to present a coherent approach for understanding the results.

2.0 SIGNAL PROCESSING

Drawing from experience both in the past and from current on-going analysis efforts involving sub-surface radars and from the literature, modern signal processing techniques have been surveyed and singled out for application to the sub-surface radar data. Particular attention was paid to those techniques that provided the possibility of improved resolution of sub-surface targets or provided an enhancement of the data display/representation.

The survey of applicable signal processing techniques covered both time and frequency domain methods. In the following text is a brief description of the techniques considered along with their characteristics.

2.1 Intensity Plotting - Magnitude of Signal. This is the current method being used for the data processing and display. The method has the advantage of being simple and easily implemented. But, disadvantages occur because of the ambiguious

nature of the displayed data. The signal transmitted by a typical short pulse radar is best represented by a 'sine-wave'. Computation of the magnitude of the signal return, and subsequent display, produces two distinct lines of almost equal intensity. Each of the lines is equivalent in resolution and thus redundant. The multiline ambiguities contribute to a confusion in measuring the depth of the soil layers.

Additional problems occur in the interpretation of the signal because of the intensity level versus amplitude scaling. If the threshold at which a solid black intensity level occurs is set very low, resolution is lost for very strong or large amplitude signals. This is equivalent to a blooming problem. If the threshold is set too high, there is the possibility of loss of lower level information. An improvement in this method can easily be accomplished by developing an algorithm for optimally setting the threshold for plotting.

2.2 Intensity Plotting - Positive/Negative Half-Wave Display. Since both lines displayed by the magnitude methods are equivalent in resolution, processing only the positive or negative half will improve the ambiguity. Theoretically both positive and negative half signals have the same amplitude, that is, if the soil layers are separated enough to be resolved by the transmitted signal. Thus, either signal can be selected for display.

Theory dictates that if the dielectric constant of the first layer is less than that of the second layer, the signal return will have the same polarity as that of the transmitted signal. On the other hand, if the dielectric constant of the first layer is greater than the second, the return signal will appear to be the inverse of the transmitted signal.

Thus, as Figure 1 illustrates, a time offset can occur in the actual measurement, which relates to an error in measurement of the depth of the soil layer if only positive or only negative data is used for display. With a waveform of 3 nanoseconds transmitted, a resolution of 18 inches is realizable. Errors in measurement of soil layer depth of 9 inches, if tolerable, would make the half-wave rectification scheme very feasible and easily implemented.

2.3 Time-Crossover With Amplitude Weighting Since the return signal (sine-wave) has both a positive and negative response with approximately equal amplitudes, this

implies that the detection of the cross-over between the positive/negative peaks could be used as a more accurate indication of signal return position, and improve resolution. Since noise will also make the signal return oscillate about zero, the presence of noise may generate cross-overs that will be detected where soil layers do not actually occur. Thresholding the noise will help this situation. But a better method involves an intensity for display which is determined by the signal amplitude averaged either side of the crossover point. An equivalent method is to use the derivative of the signal return, since as the positive/negative amplitudes increase, so does the absolute value of the derivative. The accuracy of the measurement of depth can be improved using this method according to the equation:

$$\sigma_R = \frac{\delta R}{\sqrt{S/N}} = \frac{\tau C}{2\sqrt{S/N}}$$

where:

σ_R	=	standard derivation of measurement error
δR	=	resolution in range
τ	=	pulse width
C	=	speed of light = 3×10^8 m/sec.
S/N	=	signal-to-noise ratio

The actual width of the recorded signal intensity line at the detected cross-over point should be proporitional to, σ_R, the standard deviation of the mesurement error.

2.4 Time Correlation. Standard radar techniques include cross-correlation of a replica of the transmitted signal with the return signal. For some pulse shapes this can improve the detection of signal returns and resolution properities. The signal from the short pulse radar, however, is part of a 'sine wave', and when cross-correlated with the return signal does not produce improved resolution. In addition, since most of the signal returned from the soil layers is "clutter" and not random noise, there is essentially no improvement in signal-to-noise-ratio (detectability).

Thus, the time correlation method is not significantly useful for the soil layer problem.

2.5 Synthetic Aperature Radar (SAR) Techniques. SAR is a well known technique for effectively producing improved resolution of radar data. The improvement provided by standard SAR techniques is brought about by synthesizing an increased antenna aperature, thus decreasing beamwidth, and improving spatial resolution. Several factors preclude this technique from being used effectively for the short pulse radar systems being considered.

The first stems from the fact that SAR processing involves the correlation of Doppler information to obtain a beam sharpening or synthetic aperature. The Doppler effects are not present in the soil radar data. The second, involves the fact that the short pulse radar data is collected in the near field of the antenna, where an effective beam is not yet formed.

A modified synthetic aperature technique can be used to combine the data. It involves the use of simple addition of time/depth correlated signals from sequentially taken, spatially separated measurements. Unfortunately since the soil layers are extended targets, ambiguities are created which throughly confuse the data to the point of non-recognition of soil layers. The method does work and is used in weapons locations systems, for single isolated targets, but not spatially extended target areas.

2.6 Spectral Analysis Techniques Fourier transform techniques are very useful for analysis of data containing multiple frequency reasonances. Especially when the presence of specific frequencies, and their extraction leads to identification of a particular target. In this sense the discrimination between a 'soil layer' and a 'rock', 'pipe' or other point target can be made. But it is believed that the current intensity display correlated by 'eye' can do the recognition process of point targets better than a computer algorithm using frequency analysis. The capability of a human to recognize and correlate data when properly displayed far exceeds most analysis techniques for data discrimination. Thus, the recommendation is that for the soil layer scenario, the frequency analysis techniques are not necessary and do not yield improved resolution for depth measurement or target identifications.

There is an area where frequency response can be useful; the estimation of dielectric constant and resultant soil type (density) classification. In this area, slight perturbations in the frequency characteristics can be an indication of pulse dispersion (time-elongation) and therefore be related to material dielectric constant and loss tangent. Algorithms for this approach have yet to be developed and investigated, they are not part of existing techniques.

2.7 Homomorphic Filtering A process called homomorphic deconvolution was investigated for applicability to the soil layer problem. This approach theoretically allows one to trade radar bandwidth for processing complexity. In other words, additional processing could synthetically provide greater range resolution than one could conventionally achieve with a given radar system. A brief investigation of this technique has lead to some preliminary conclusions. These conclusions and a description of the process are given below.

Functionally, homomorphic deconvolution accomplishes the same task as inverse filtering, it accentuates the extremeties of the spectrum to yield a larger bandwidth. Inverse filtering is illustrated in Figure 2. The spectra of the signal at the input and output of the inverse filter is illustrated in Figures 2 (a) and (d). The inverse filter is designed to have a frequency response which is the inverse of the fundamental component of the input spectrum as illustrated in Figures 2 (b) and (c). In this filtering process, it is assumed that the information of interest is the smaller, faster varying component of the input spectrum which is preserved in the inverse filtering process. In a radar application where a transmitted signal is reflected from multiple surfaces or points extended in range (or depth for soil layer), the slowly varying spectra component represents the transmitted signal spectra while the faster, more rapidly varying component yields information about the separation between layers. It is this latter information which is of interest and which is preserved in the inverse filtering process.

One of the problems in using inverse filtering is that the portion of the input spectrum which represents the transmitted signal must be known precisely, including magnitude, in order to perform inverse filtering. The output of this type of filter is very sensitive to filter mismatch. Thus, in practice, the theoretical performance of inverse filtering is seldom achieved.

One of the proported advantages of homomorphic deconvolution is that the transmitted signal does not need to be known. The process separates the radar return spectrum into two parts, that part representing the transmitted signal and that portion which yields information about scatterer position. The equivalent operation in the time domain is called deconvolution. Radar returns can be mathematically represented by the convolution of the transmitted temporal signal with a series of point or plane scatterers represented by impulse functions. If we can successfully deconvolve the transmitted signal and the impulse functions, then the range resolution has been enhanced and is theoretically zero.

The non-linear process called homomorphic deconvolution is illustrated in Figure 3 where the transmitted signal is denoted by x(t) in the time domain and $S(e^{jw})$, in the frequency domain. The response h(t) is the impulse function representing the point scatterer distribution in time or range. The radar return is denoted as y(t) and $Y(e^{jw})$, respectively. As indicated in Figure 3, the process involves the use of the forward and inverse Fourier transform F and F^{-1}, respectively. The complex natural logarithm and inverse natural logarithm (exponential) is also utilized. The time domain function formed by the logarithmic process is called the cepstrum. Several types of linear filtering can be used in the cepstrum domain to separate x'(t) and h'(t), which are non-linear versions of x(t) and h(t). The filtering technique often used is to simply low-pass and high-pass filter; that is, dividing y'(t) at some convenient value of t as shown in Figure 3. Each of these components of y'(t) are then transformed back into the frequency and time domains by an inverse non-linear process. The result is a deconvolution if h'(t) and x'(t) are separable in the cepstrum domain. This depends somewhat on the separation and relative amplitude of the scatterers. The deconvolved components x(t) and y(t) are shown in Figure 3.

In practice, the deconvolution process just described is not as simple as it sounds. One must be careful to insure that the logarithmic transformation provides a unique transformation. A process not indicated in Figure 3, called "phase unwrapping" must be performed. The complex log function is module 2π in its imaginary component which component also represents the phase variation of the frequency spectrum. Thus, the imaginary component must be "unwrapped" so that it is not module 2π. In addition to this special consideration, one must also remove the linear component of the spectrum phase before transforming into the cepstrum

domain. This linear phase must be replaced after the divided cepstrums are transformed back into the frequency domain. A flow diagram which itemizes the functions to be performed in the homomorphic deconvolution process is shown in Figure 4. In this diagram, only the high-passed portion of the cepstrum is processed since only the scatterer distribution is of interest. Detailed discussions concerning the practical considerations of homomorphic deconvolution are given in References 1 through 17.

Some results of the deconvolution program on synthetic data are shown in Figures 5 and 6. In Figure 5(a), it is assumed that two unequal size scatterers separated in range reflect a transmitted pulse. The second return is one-half the amplitude of the first return. The spectrum of this composite radar return is shown in Figure 5(b). The period of the rapidly varying component of this spectrum is inversely proportional to the separation of the two scatterers. The slowly varying component of the spectrum is the spectrum of the transmitted waveform. The upper portion of the cepstrum is shown in Figure 5(c); the lower portion has been eliminated. The deconvolved return is shown in Figure 5(d). Note that the time spread (resolution) of the two returns is smaller than in Figure 5(a). Thus, the resolution has been increased via this process.

Figure 6 depicts a similar situation except the second radar return is now almost as large as the first. The point to be made in this example is illustrated in Figure 6(c). Note that a decaying train of impulses occurs in the cepstrum domain. The rate of decay depends on the relative size of the two radar returns. If the two returns are equal in amplitude, the impulse train in the cepstrum domain does not decay but consists of an infinite number of impulses of equal amplitude. If the second radar return is larger than the first, the impulse train in the cepstrum domain diverges without limit. Since, in practice, the second return can easily be larger than the first, one must consider ways of solving this processing problem. One approach is to weight the radar return response to force the second return to be smaller than the first and then later remove the weighting factor.

The foregoing example considered was for a simple two scatterer problem. If more scatterers are considered, the process could become more complicated in a practical application.

2.8 Spatial Averaging - Within Beam. Signal amplitude modulations are caused by addition of signals in and out of phase due to the scattering from extended targets. This makes the 'soil layer' signal return appear to be changing in depth (range) more rapidly than the layers really are, or possibly appear to not exist over some areas. This effect can be smoothed out with no loss of information or resolution,by averaging signal returns over a short spatial extent. This averaging will depend upon the rate that the data is taken and the speed that the radar is moving across the ground. The general rule is that the number of pulses recorded within the cross-range extent of a beamwidth can be averaged.

3.0 THEORETICAL MODELLING

The signal from the short pulse radar used for soil layer measurements is closely approximated by a single cycle of a 'sine-wave' with slight leading and trailing ringing effects included. This basic signal shape was actually measured on the short pulse radar in use at Georgia Tech. The characteristics of several signals are given in the table below.

TABLE 1
SIGNAL CHARACTERISTICS

BANDWIDTH	SIGNAL PULSE LENGTH	RESOLUTION
1 GHz	1 nanosecond	.15 M
330 MHz	3 nanosecond	.45 M
100 MHz	10 nanosecond	1.5 M

The relationships are

$$\delta R = \frac{C \cdot \tau}{2} = \frac{C}{2\,BW}$$

where:

SR = range/depth resolution (meters)

C = speed of light = 3×10^8 M/S

τ = pulse length (sec)

BW = bandwidth (Hz)

3.1 Soil Layer Model. The soil layers were modeled as infinite layers of uniform dielectric medium, stacked on top of one another. For the simulation, it sufficies only to examine one boundary transition and this is illustrated in Figure 7. The shape, as indicated, can be specified as a parabola in one axis while infinite in the other axis (essentially a parabolic surface).

The signal returns are computed at each measurement position of the radar over all angles within plus and minus one full beamwidth of beam center. The beam center is always pointing straight down (perpendicular to the surface layer) and the measurement position is always incremented along the varying parabolic surface as indicated in Figures 8. At each position signal returns are summed for all angles. Each signal return at a given angle is a function of the loss through the medium, the reflection coefficient from the layer and the antenna beam shape factor. The antenna beam shape factor is assumed to be of sin (x)/x functional form. The reflection angles for the signal are geometrically calculated and the reflection coefficient computed. The medium loss factor is an input by the user.

3.2 Target Model. Only one specific target was modelled, that of a pipe. Figure 9 illustrates the situation. Here, as in the layer model, the size, depth and dielectric constant of the pipe is user specified. The program then computes the signal return at each measurement position based upon the beamshape, reflection coefficient and loss through the medium.

3.3 Signal Simulation. In the following, the results for the simulation of return signals for a short pulse radar are illustrated. The first set of plots is for a parabolic soil layer boundary. The results illustrate the effects of beamwidth and pulse length on the overall measurement capability. The second set of plots illustrate the results of simulation for a 'pipe' target.

The physical situation for the soil layer simulation is given in Figure 10. The layer boundary has its peak one meter below the surface. Measurements are computed from $\pm$ 0.5 meter around this peak in 0.05 meter increments. The

angle data includes signals from $\pm$ 1.0 radian in the X-axis and $\pm$ 0.5 radian in the Y-axis, covering the symmetrical beamwidth in each case. Figures 11-13 illustrate the signal returns plotted in a position sequential manner for cases where the beamwidth is 0.5, 0.3 and 0.1 radians. Examining Figure 11 first, several important facts are apparent. The large signal return, which occurs first in time, is due to the signal ray from the antenna at an angle such that the ray strikes the boundary at or near perpendcuilar incidence. This is the largest signal return because the reflection coefficient is the greatest, and it is first in time of occurance because it is the minimum distance to the boundary. The next signal return seen in time is a reflection from other angles, with the largest seen to be at an angle looking straight down. Thus, the actual boundary is defined by the lower magnitude set of signals seen further out in time of occurance. The large signal returns portray a fictitious synthetic layer boundary. If the depth of the layer boundary is measured using this large signal return, errors will result. Clearly the flatter the boundary the closer the real layer return is to the fictitious layer (normal incidence) return.

As Figures 12 and 13 are examined, it becomes apparent that a smaller beamwidth reduces the area of large normal incidence returns and the layer boundary becomes well defined, unambiguously. This clearly points out the need for investigation of methods for achieving narrower beamwidths.

Figures 14-17 illustrate the application of various signal processing techniques to the data simulation of Figure 11. Figure 14 plots the magnitude of the signal return and this is basically the processing currently implemented with the SIR system. From examination it is obvious that on an intensity type plot, multiple parallel line would occur. This result leads to confusion in interpretation of layer depth. Figure 15 uses the positive signals only, and clearly improves the interpretation situation. Figure 16 uses the negative signals only, and even this provides possible improvement in interpretation. Figure 17 is the result of a time cross-correlation of the return signal with a replica of the transmitted signal. As expected a significant improvement is not in evidence.

Figure 18 illustrates the signal returns from a 'pipe' like target. The processing techniques are applied to the basic signal returns in Figures 19-20. The pipe diameter is very small (1cm) and the signal returns at each position are mainly the normal incidence reflection. Thus, an isolated target of this nature appears to

yield an extended boundary-like return signal character. This of course can be distinguished from an extended layer boundary by noting the lack of multiple false boundary layer returns, as indicated in Figure 11.

The effects of a narrower beamwidth would be to produce a more isolated location measurement for the single target case. As for the extended boundary layer case, the narrower beamwidth can improve the depth measurement process.

The effects of shorter transmitted pulse lengths upon the return signal is to directly improve the resolution of the system. But, this resolution can be 'spoiled' or lost due to a large beamwidth dispersion effect. This is illustrated in Figure 21, where there are reflected signals from a horizontal boundary layer. Assumming that an extremely short pulse is transmitted, there will be signal returns from a continuum of angles across the beam. These signals will be modified in amplitude by the reflection ioefficient and beam shape factor, but do arrive at the antenna at different delay times. These signals when added together produce the effect of lengthening the return pulse shape, and thus decreasing the resolution. The result of this analysis is that beamwidth again becomes a significant factor in determining system performance.

4.0 DATA DIGITIZING AND EDITING

The entire NASA supplied analog tape was digitized during the term of the study. Hardware problems were encountered during several initial attempts, but were fixed, and digital tapes produced. There were several tracks of data on the tape and over 500,000 individual signal returns were digitized. With this amount of data, and the funding allotted, no attempt was made to plot all of these signal returns. NASA supplied original intensity plots were also used for data editing and investigation. In fact, these plots when directly compared with the simulated returns provided the verification of the theory.

It must be pointed out that difficulty was encountered when attempting to synchronize the signal return length via the digitized data. Pattern recognition techniques were employed to verify the start of the signal return, but many erroneous trigger points were observed. This time synchronization problem significantly complicates the processing of data efficiently.

As a result, the plotting and display of significant amounts of measured data was not attempted. It was felt that the time involved could be better spent on the theory and processing techniques.

5.0 SIGNAL PROCESSING APPLICATIONS

For the purpose of illustration of techniques, and given the problems developed in attempts to synchronize the digitized data, the plots in this section are not time synchronized. This, nevertheless, does not detract from the results that can be achieved utilitizing the signal processing methods.

Figures 22-27 illustrate an original section of data and processed sections using the magnitude, positive signal and negative signal methods.

Many more individual short sections of data were processed with the results being identical, and as expected, according to the simulation. To provide a comparison between the NASA supplied intensity plots and the processing techniques, the processed data should be plotted in a similar manner. Although this process was available for the digitized data, the time and funding for the study precluded this action. Instead of continuing to sort through small sections of digitized data, it was felt that the time could be better spent more fully analyizing the simulation results and processing methods.

6.0 CONCLUSIONS

The key results of this study point out that there are simple methods for processing and display that can improve data interpretation. These improvements can possibly be more helpful than more complex techniques to improve resolution synthetically.

Depth resolution or thickness measurement can be directly improved by shortening the pulse length. But, antenna beamwidth can cause this resolution to be not realized in the measurement of certain extended layer boundaries. Thus, another key conclusion of this study is that decreasing the beamwidth can improve the data display and interpretation as much as shortening pulse length in layer boundary measurement applications. The derivative-zero-crossing method of signal processing results in possible improvement in the accuracy of layer boundary or

single target depth. This improvement is proportional to signal-to-noise ratio of data.

For isolated small targets such as pipes or rocks, resolution can be improved by complex processing techniques such as homomorphic filtering and simplified synthetic aperture processing. It also is suggested that methods for correlating the frequency spectra results with soil dielectric constant should be investigated further.

In addition, to fully compare the digital data improvements, a significant amount of manpower would be expended in creating an identical plot to that of the original intensity chart recording. It is suggested that some of the simple processing techniques be implemented in analog hardware. The analog signal can then be recorded on a system identical to the original chart recorder. Easy comparison will then be available.

The actual design and fabrication of some of the simple processing techniques should be underaken as a minimum of further efforts in this area of soil radar response studies. Also, there should be a continuing effort of signal simulation so that a better understanding of soil layer signal returns can be developed for more complex situations.

REFERENCES

1. "Detection and Estimation of P-PP Delay Time by Cepstrum Analysis," Transactions-American Geophysical Union, Volume 57, Texas Instruments, Inc., 1976, p. 963.

2. Chen, C. S., Roemer, L. E., and Grumback, R. S., "Power Cable Diagnostics Using Cepstrum Processing of Time Domain Reflectometry," IEEE Transactions on Power Apparatus and Systems, Volume 95, 1976, p. 1762.

3. Hammond, J. K. and Peardon, L. G., "Power Cepstrum Applied to Multi-Peaked Wavelets," Journal of Sound and Vibration, Volume 48, 1976, pp. 537-541.

4. Poche, L. B. and Rogers, P. H., "Echo Reduction in Low-Frequency Calibration Using Complex Cepstrum," Journal of the Acoustical Society of America, Volume 60, 1976, p. 25.

5. Hassab, J. C. and Boucher, R., "Probabilistic Analysis of Time-Delay Extraction by Cepstrum in Stationary Gaussian Noise," IEEE Transactions on Information Theory, Volume 22, 1976, pp. 444-454.

6. Zimdars, M. A., Taylor, R. W., and Willis, D. E., "Application of Cepstrum Analysis to Discrimination of Multiple Arrivals at First Zone Distances," Transactions American Geophysical Union, Volume 57, 1976, p. 85.

7. Fjell, P. O., "Use of Cepstrum Method for Arrival Times Extraction of Overlapping Signals Deu to Multipath Conditions in Shallow-Water," Journal of the Acoustical Society of America, Volume 59, 1976, pp. 209-211.

8. Mitchell, S. K. and Bedford, N. R., "Long-Range Sensing of Explosive Source Depths Using Cepstrum," Journal of the Acoustical Society of America, Volume 58, 1975, p. 20.

9. Hassab, J. C., "Network Function Theory and Complex Cepstrum," Journal of Sound and Vibration, Volume 41, 1975, pp. 127-128.

10. Hassab, J. C., and Boucher R., "Analysis of Signal Extraction, Echo Detection and Removal by Complex Cepstrum in Presence of Distortion and Noise," Journal of Sound and Vibration, Volume 40, 1975, pp. 321-335.

11. Smith, R. G., "Cepstrum Discrimination Function," IEEE Transactions on Information Theory, VIT 21, 1975, pp. 332-334.

12. Rom, R, "Cepstrum of Two-Dimensional Functions," IEEE Transactions on Information Theory, VIT 21, 1975, pp. 214-127.

13. Bohme, J. F., Cepstrum as a Generalized Function," IEEE Transactions on Information Theory, VIT 20, 1974, pp. 650-653.

14. Stoffa, P. L., Buhl, P., and Bryan, G. M., "Cepstrum Aliasing and Calculation of Hilbert Transform," Geophysics, Volume 39, 1974, pp. 543-544.

15. Hassab, J. C., "Convergence Interval of Power Cepstrum," IEEE Transactions on Information Theory, VIT 20, 1974, pp. 111-112.

16. Tribolet, J. M., "New Phase Unwrapping Algorithm," IEEE Transactions Acoustics, Speech, and Signal Processing, Volume 25, MIT Dept. of Elect. Engn. and Comp., pp. 170-177.

17. Skinner, D. P., Real-Time Composite Signal Decomposition, University of Florida, Gainesville, FL.

18. Childres, D. G., Modern Spectrum Analysis, IEEE Press

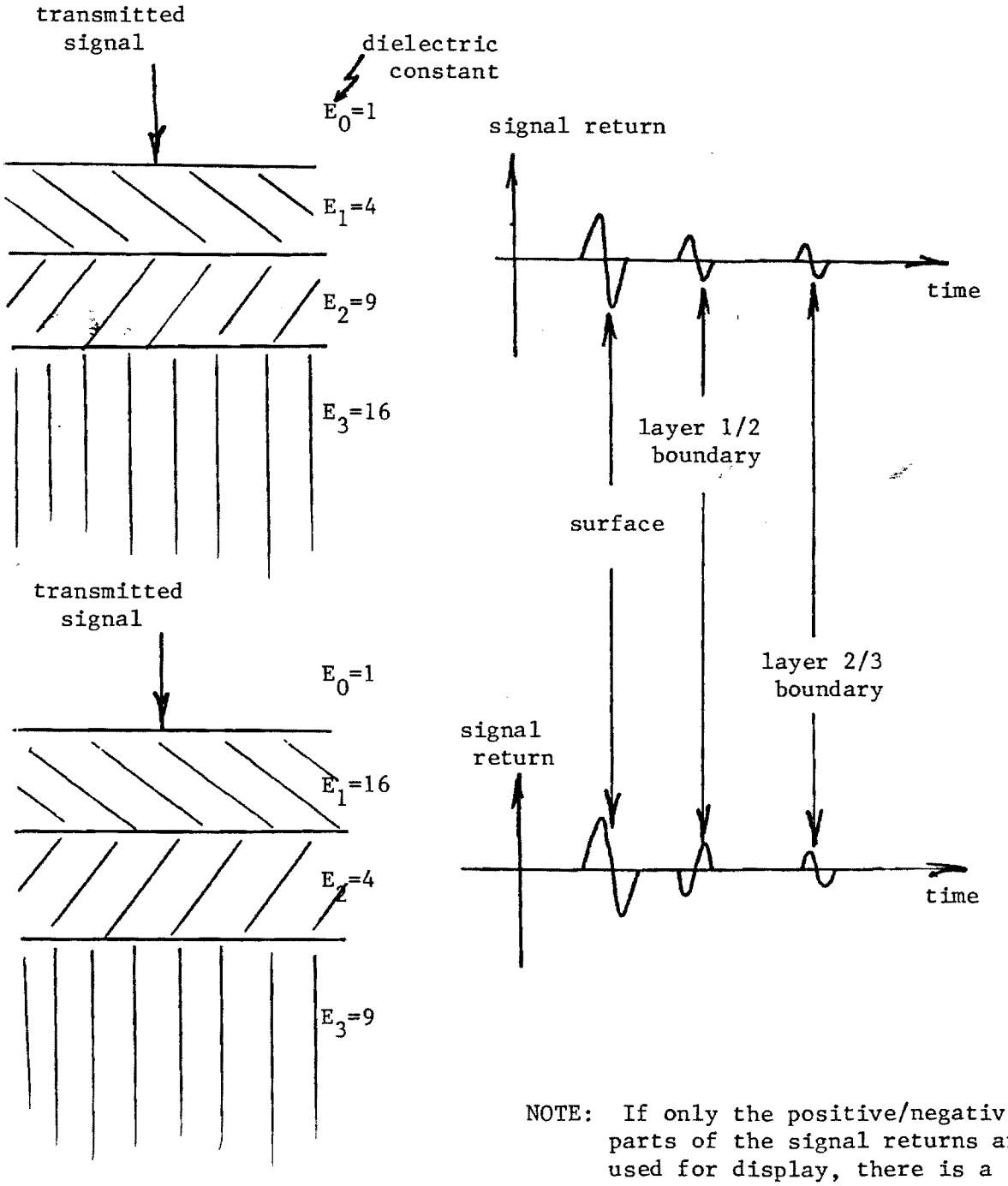

NOTE: If only the positive/negative parts of the signal returns are used for display, there is a possibility of having a bias on the layer depth calculation.

FIGURE 1 POSITIVE/NEGATIVE BIAS PROBLEM

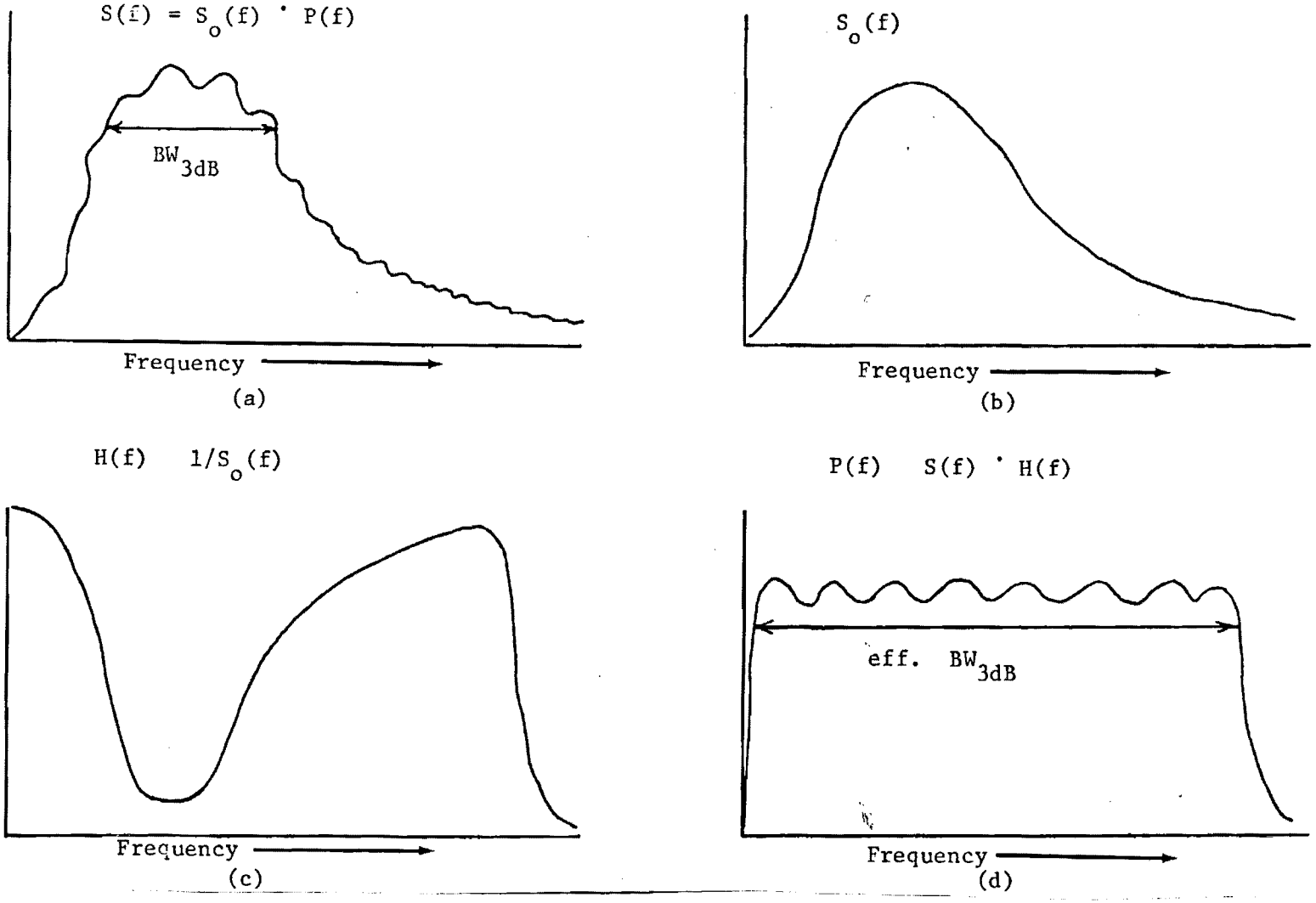

FIGURE 2 INVERSE FILTERING

(a) spectrum before filtering; (b) an estimate of the fundamental component of the spectrum; (c) the inverse filter response; and (d) the spectrum at the output of the inverse filter.

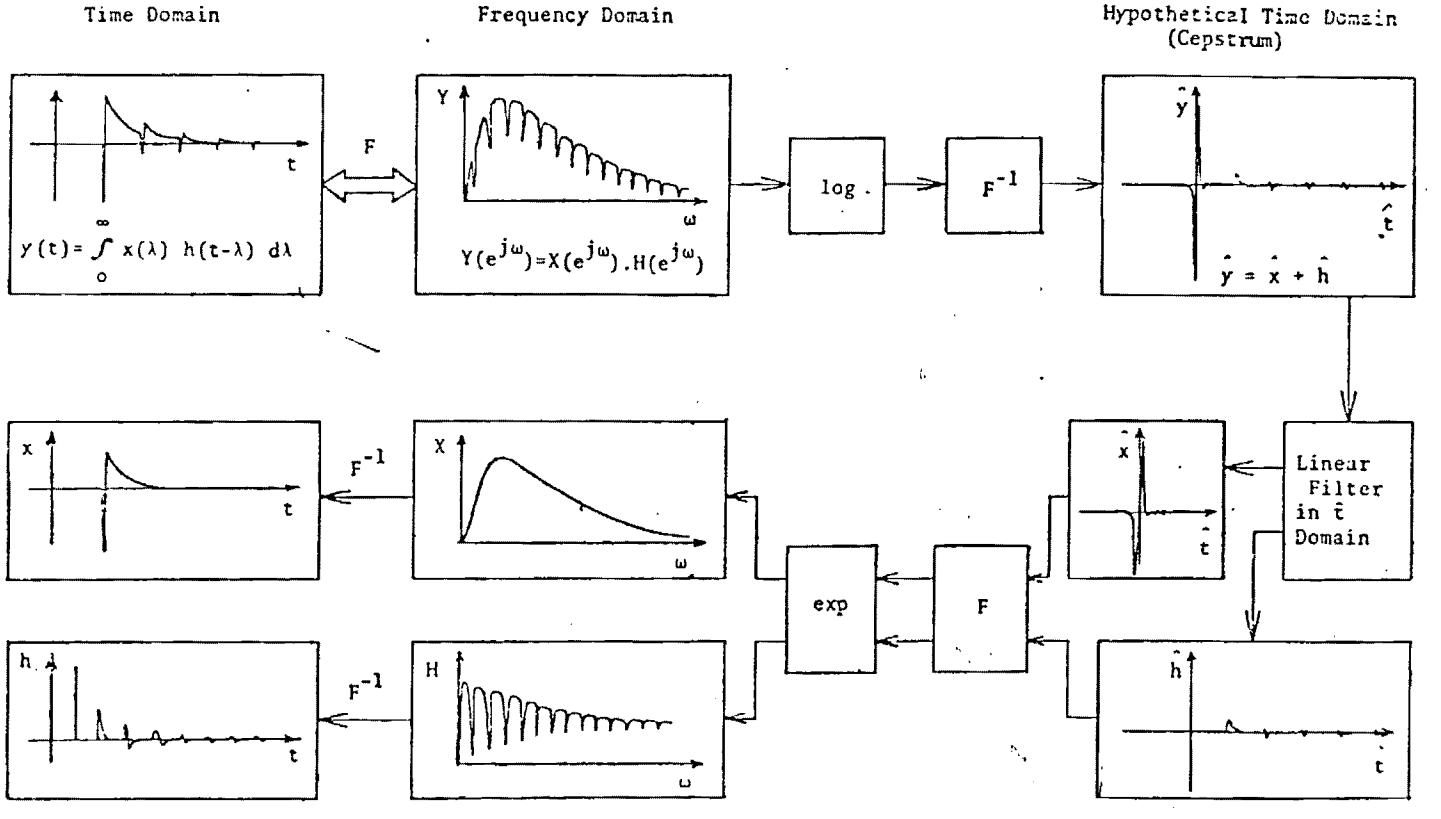

FIGURE 3 HOMOMORPHIC DECONVOLUTION

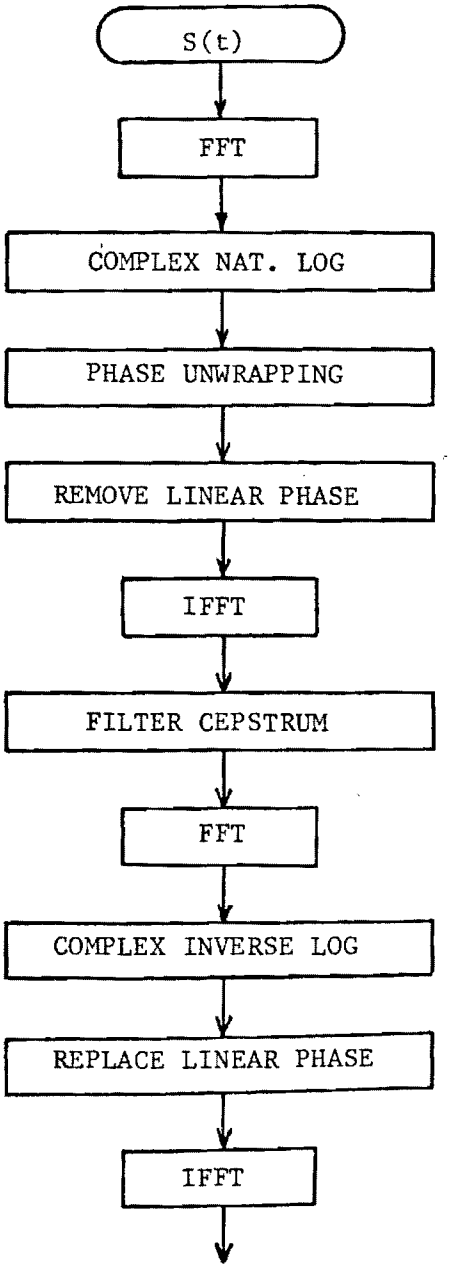

FIGURE 4 FLOW DIAGRAM

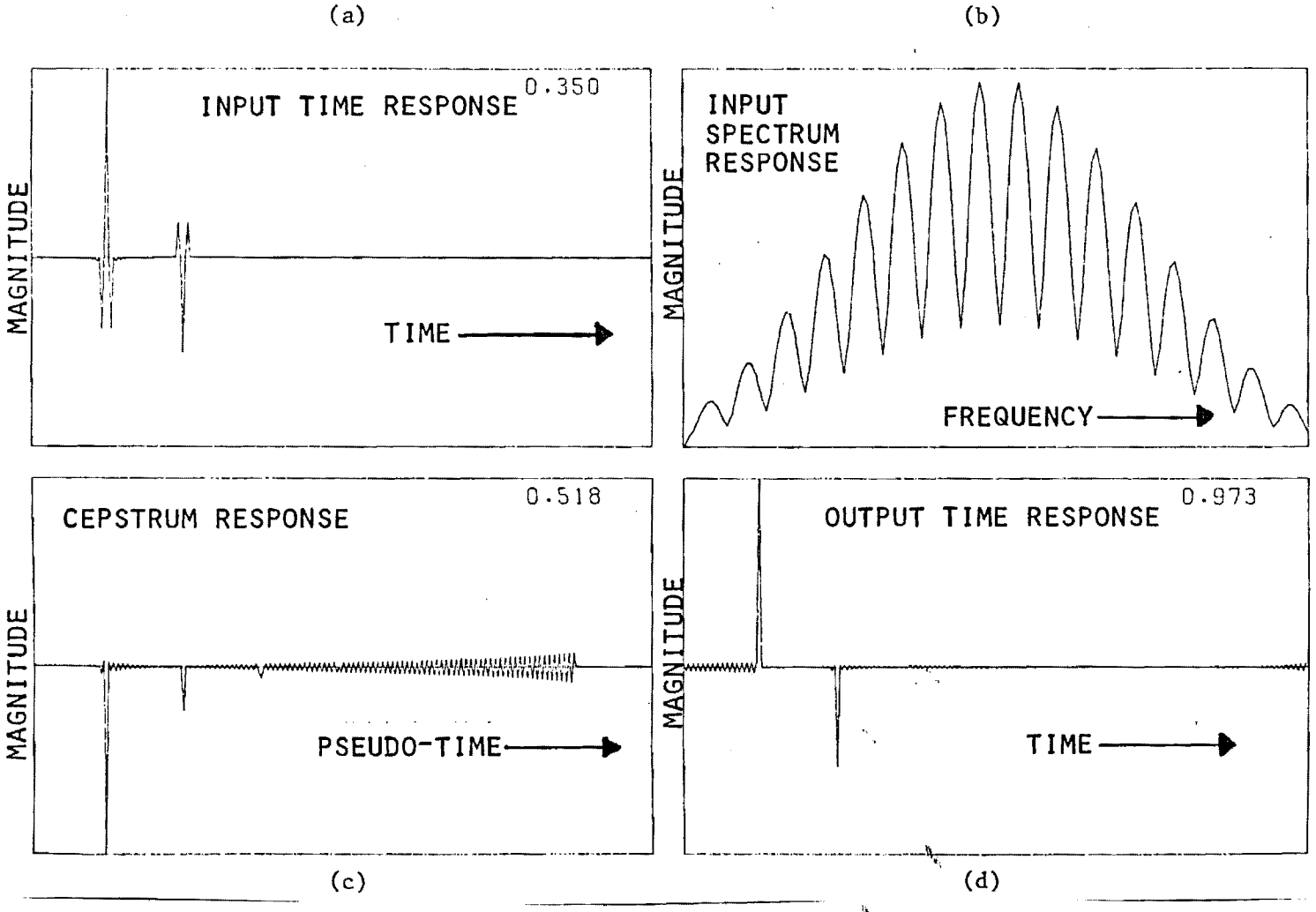

FIGURE 5 HOMOMORPHIC DECONVOLUTION, EXAMPLE 1

Results of deconvolution on synthetic data where the second scatterer is one-half the size of the first.

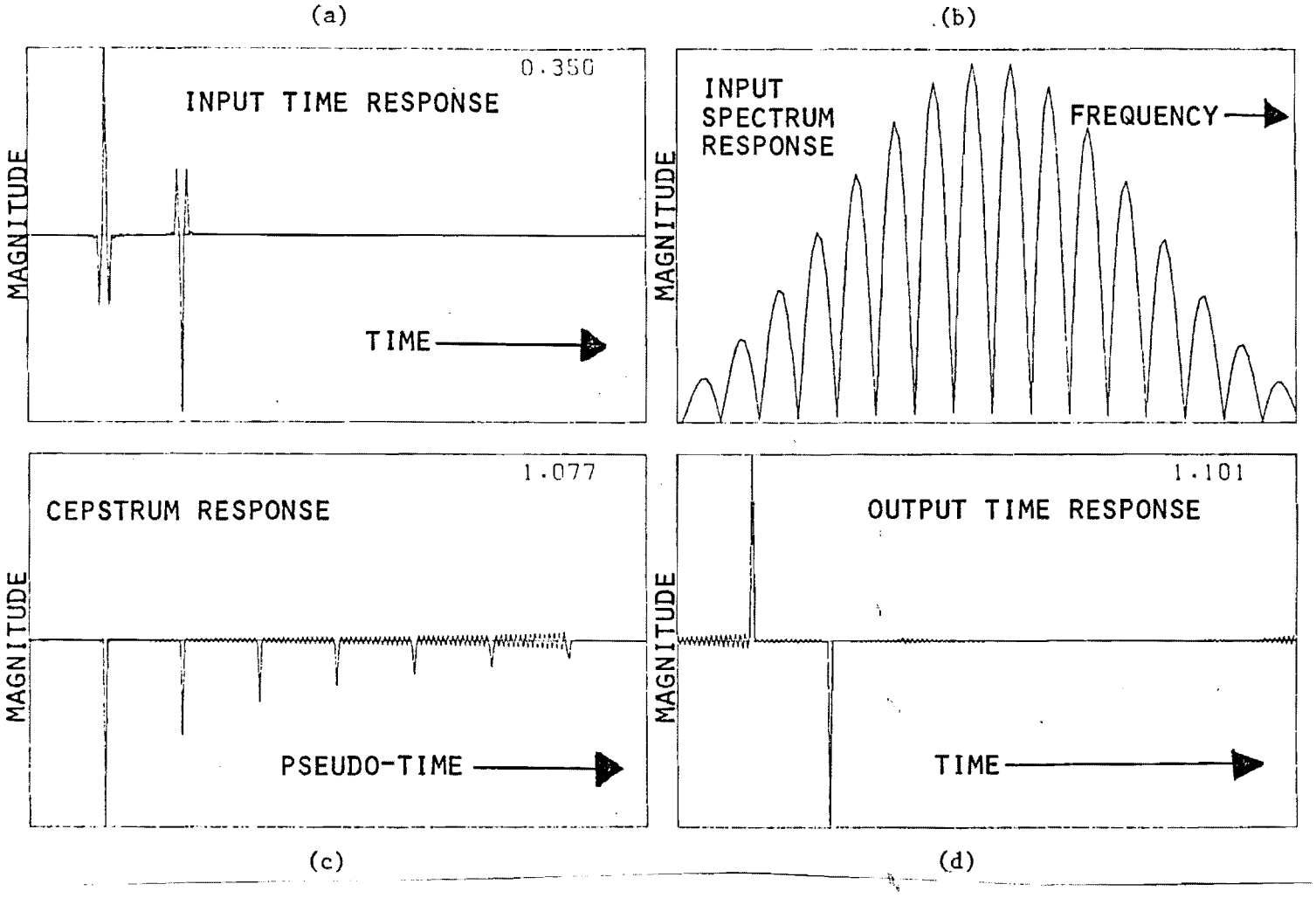

FIGURE 6 HOMOMORPHIC DECONVOLUTION, EXAMPLE 2

Results of deconvolution on synthetic data where the second scatterer is 95% of the size of the first.

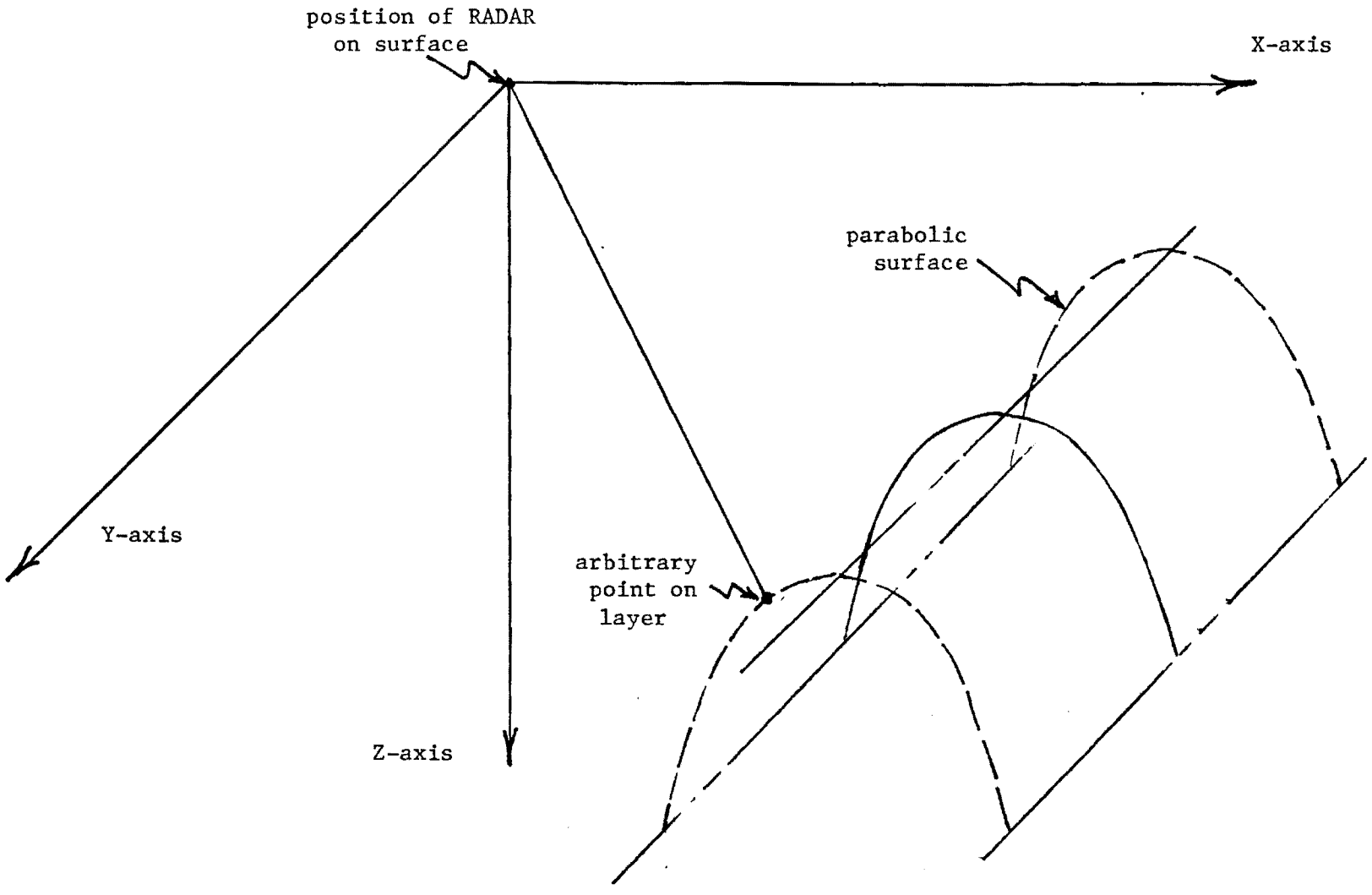

FIGURE 7 SOIL LAYER - PARABOLIC SHAPE

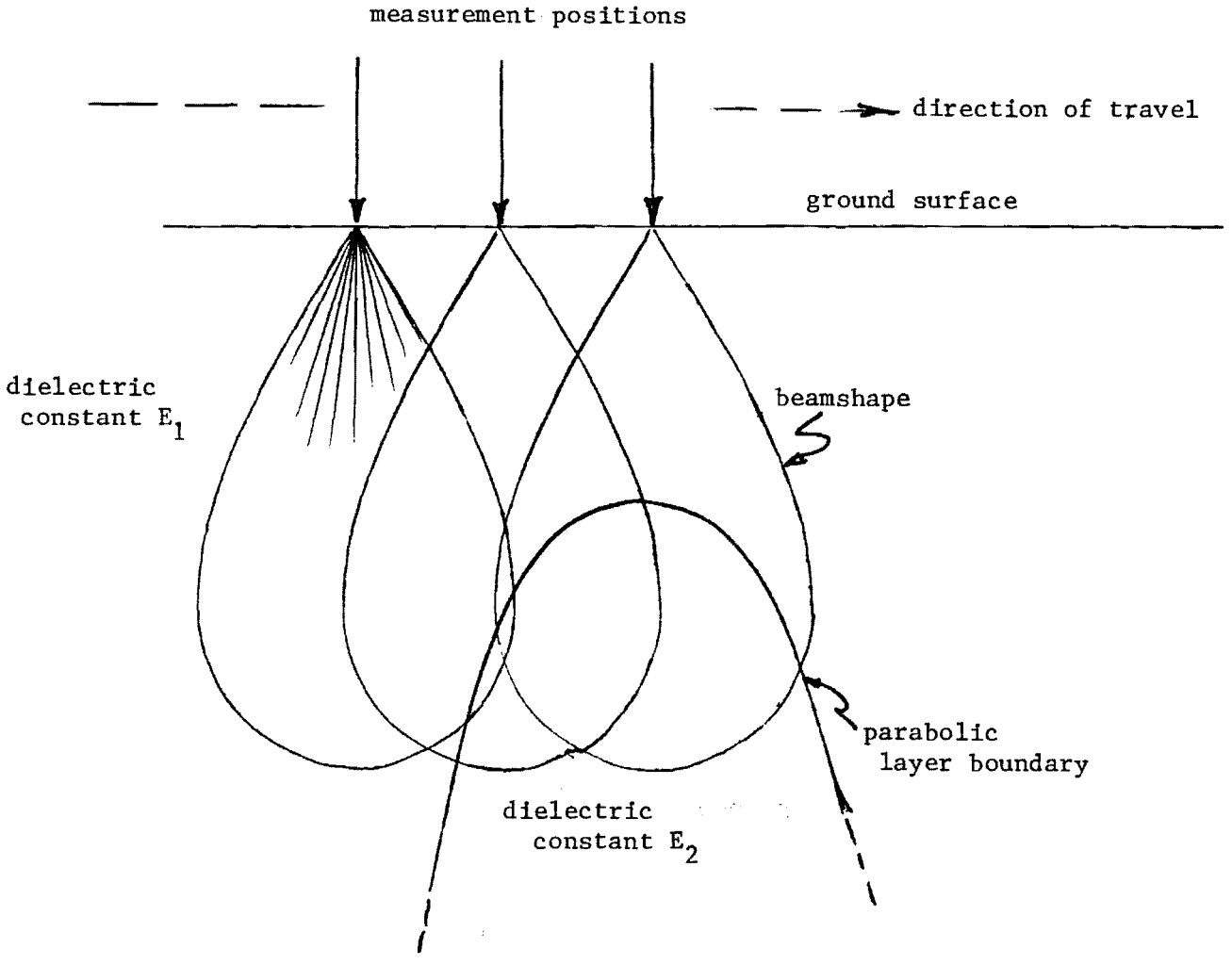

FIGURE 8 MEASUREMENT SYSTEM CONFIGURATION

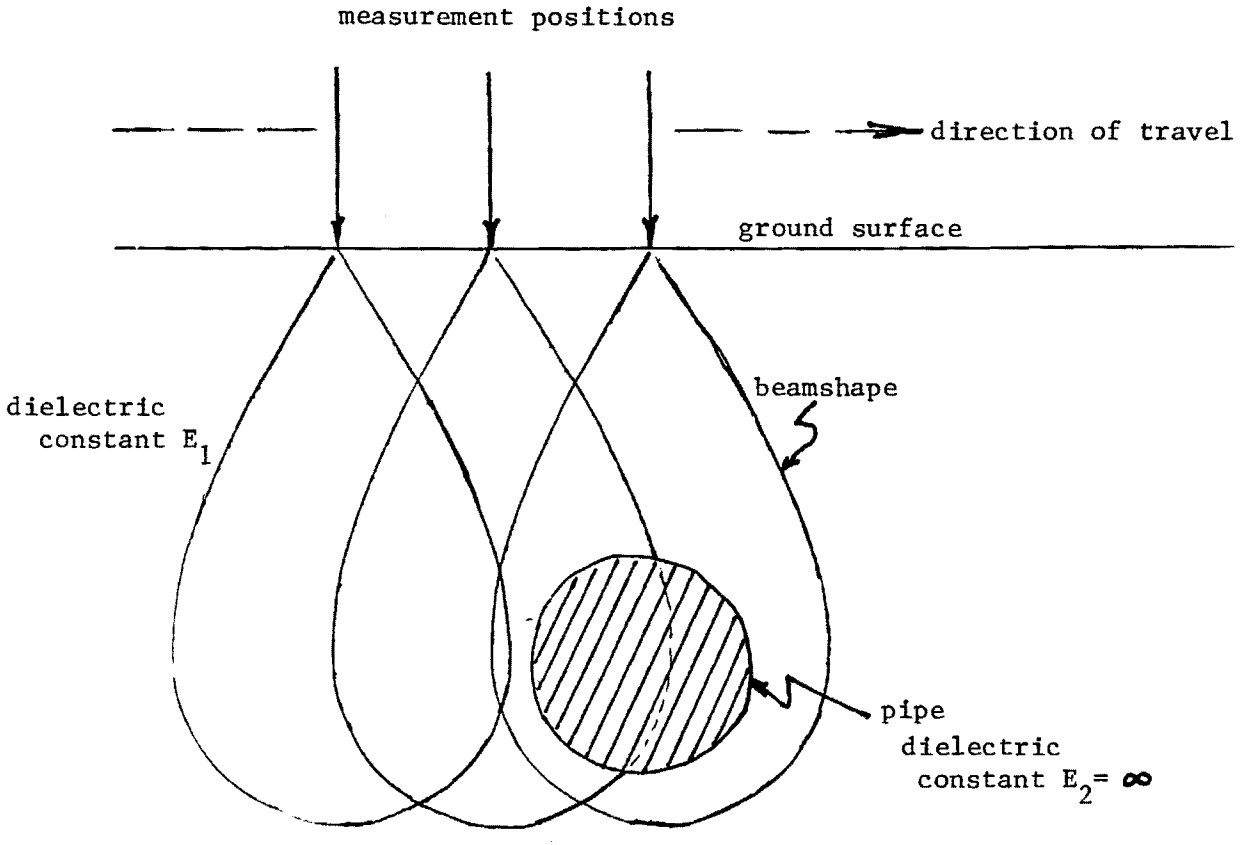

FIGURE 9 'PIPE' TARGET MEASUREMENT CONFIGURATION

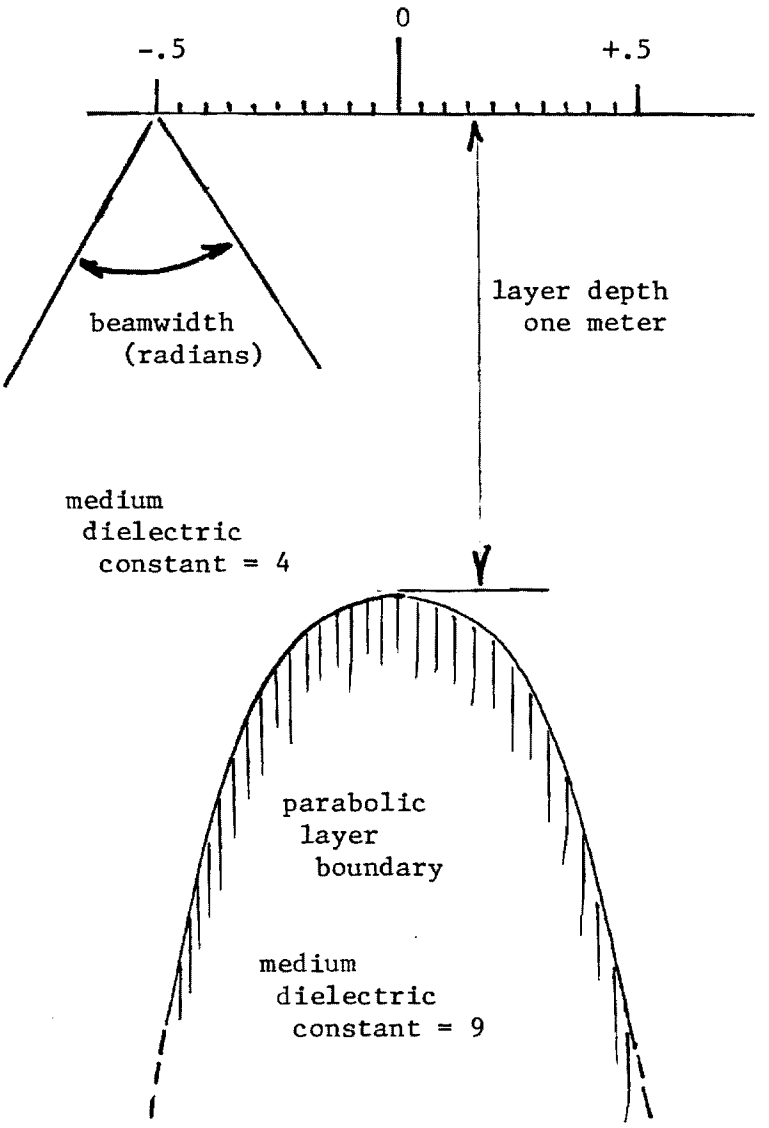

FIGURE 10 SIGNAL SIMULATION DETAIL

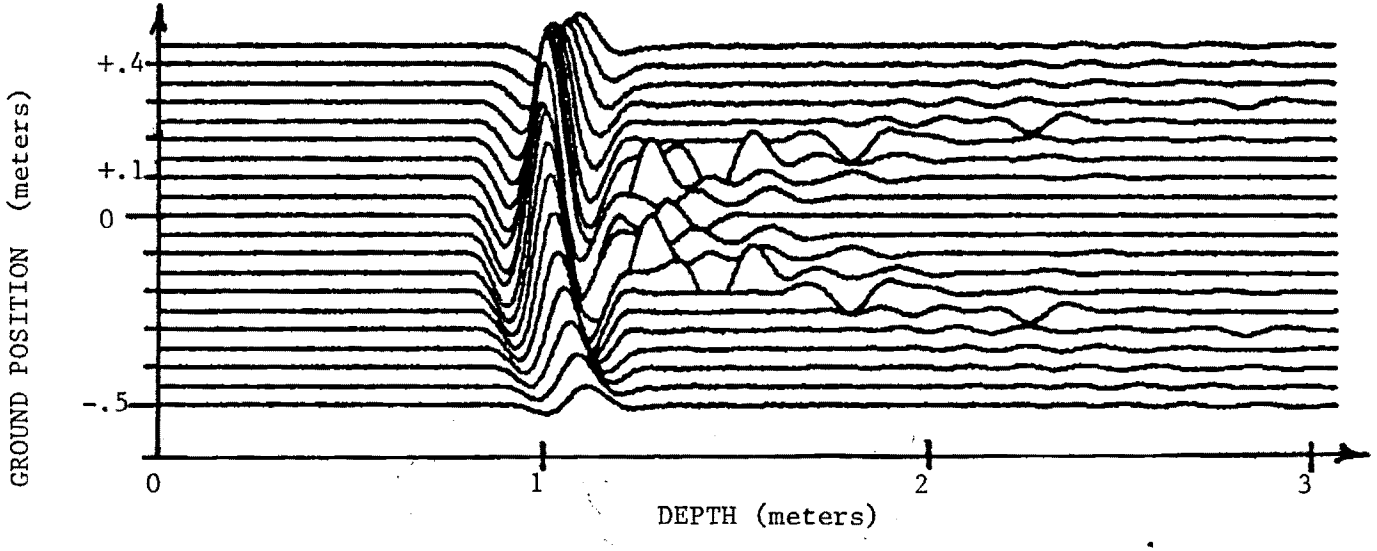

FIGURE 11 PARABOLIC LAYER SIGNAL RETURNS

beamwidth = 0.5 radians

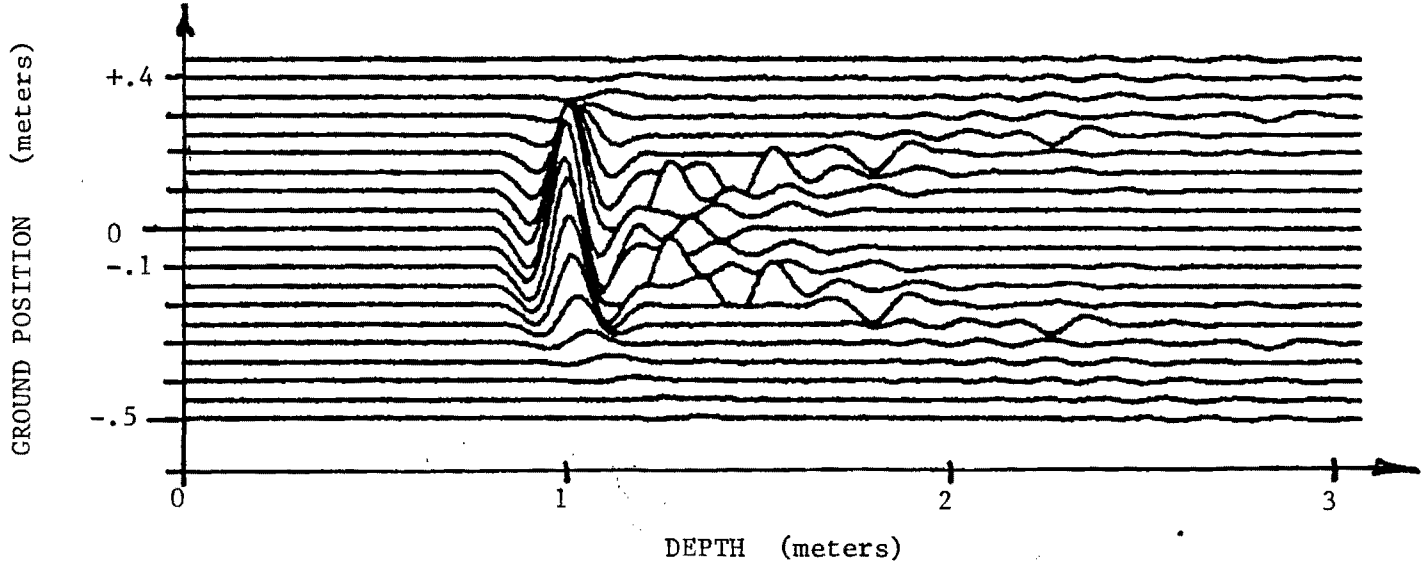

FIGURE 12 PARABOLIC LAYER SIGNAL RETURNS

beamwidth = 0.3 radians

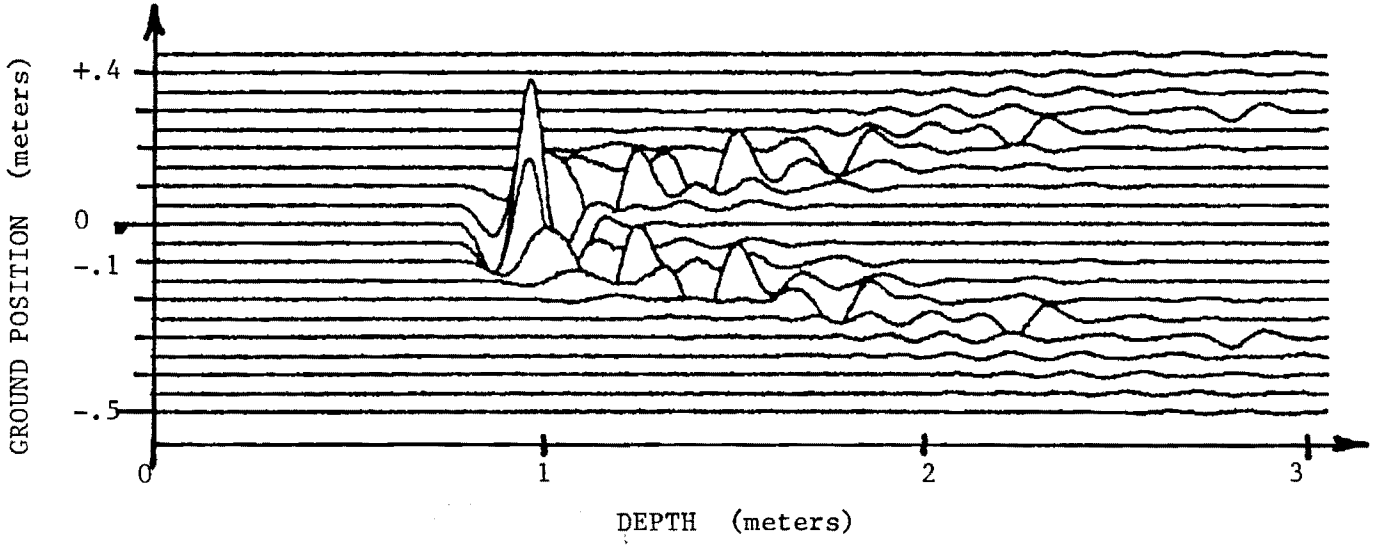

FIGURE 13 PARABOLIC LAYER SIGNAL RETURNS

beamwidth = 0.1 radians

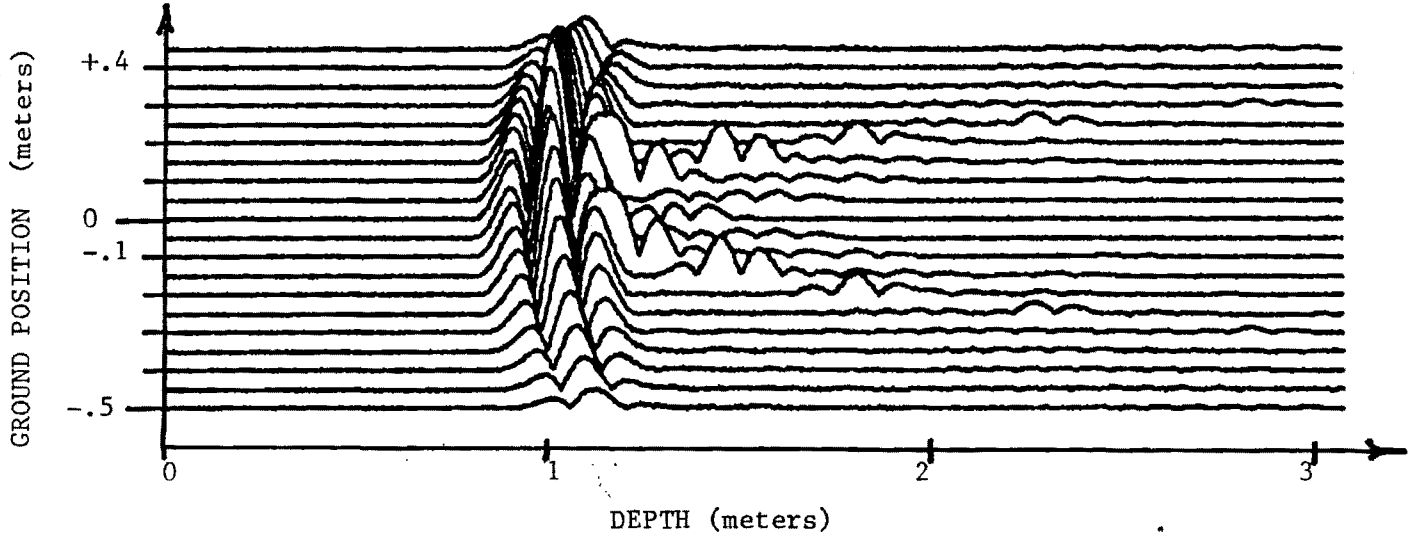

FIGURE 14 PARABOLIC LAYER - MAGNITUDE PROCESSING

beamwidth = 0.5 radians

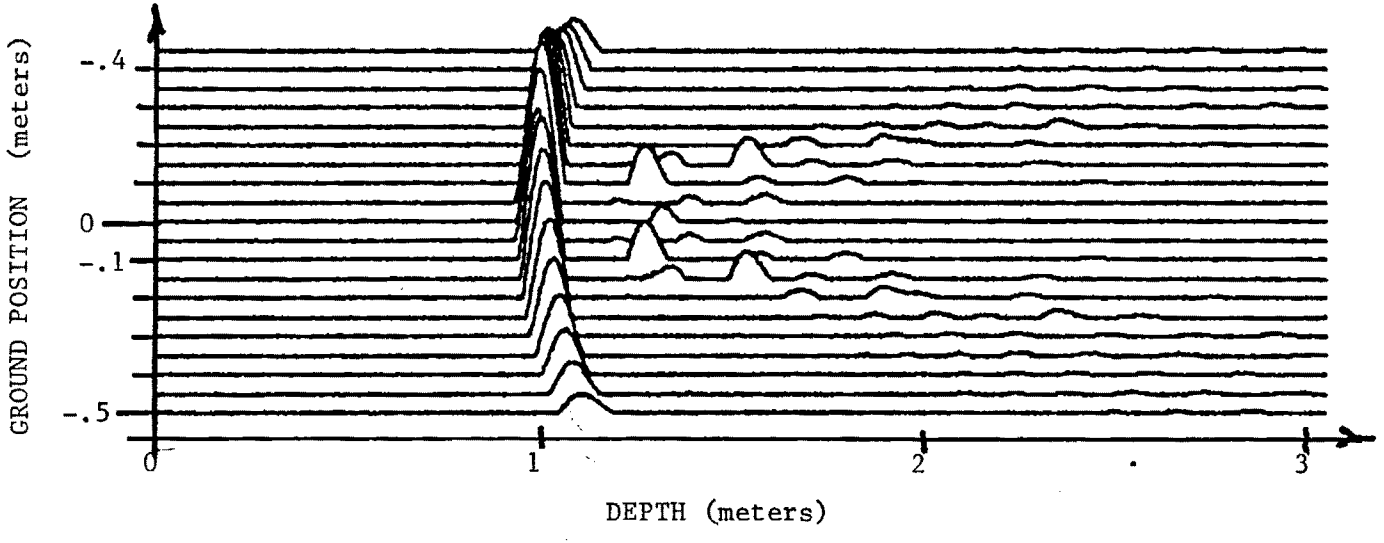

FIGURE 15 PARABOLIC LAYER - POSITIVE SIGNAL

beamwidth = 0.5 radians

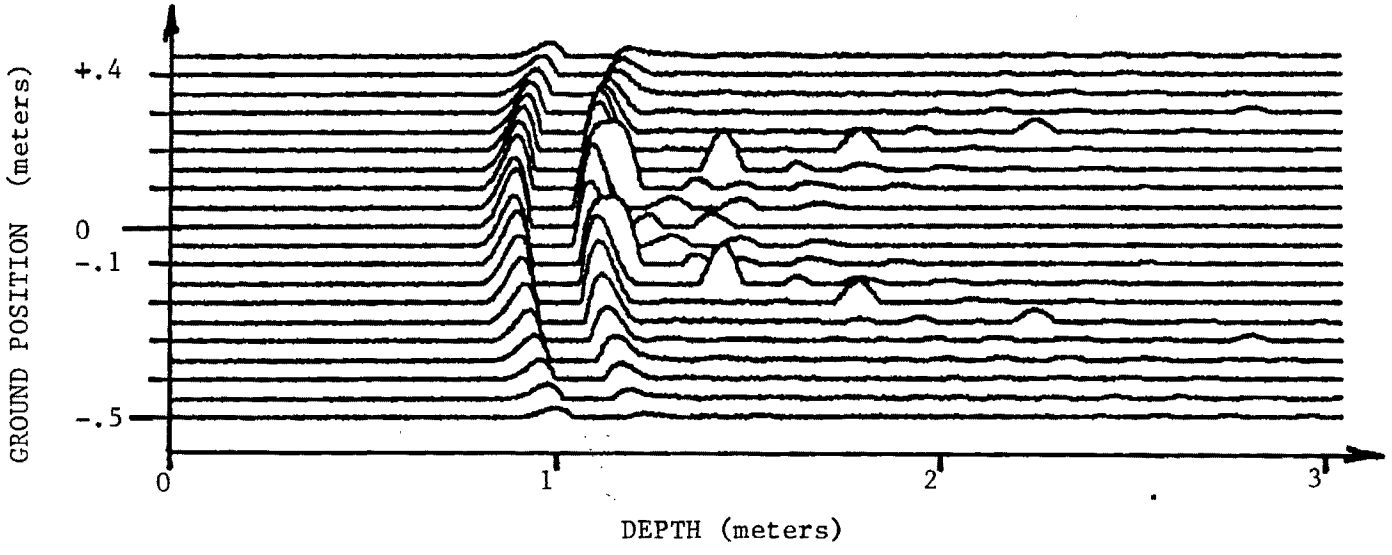

FIGURE 16 PARABOLIC LAYER - NEGATIVE SIGNAL

beamwidth = 0.5 radians

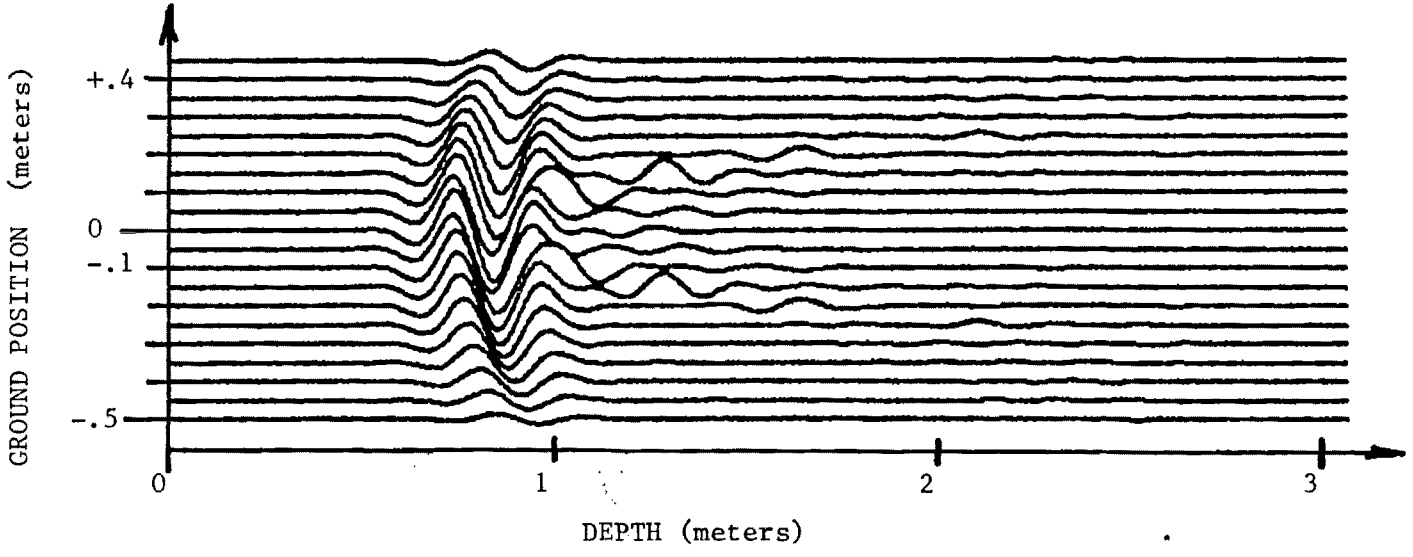

FIGURE 17 PARABOLIC LAYER - TIME CORRELATION

beamwidth = 0.5 radians

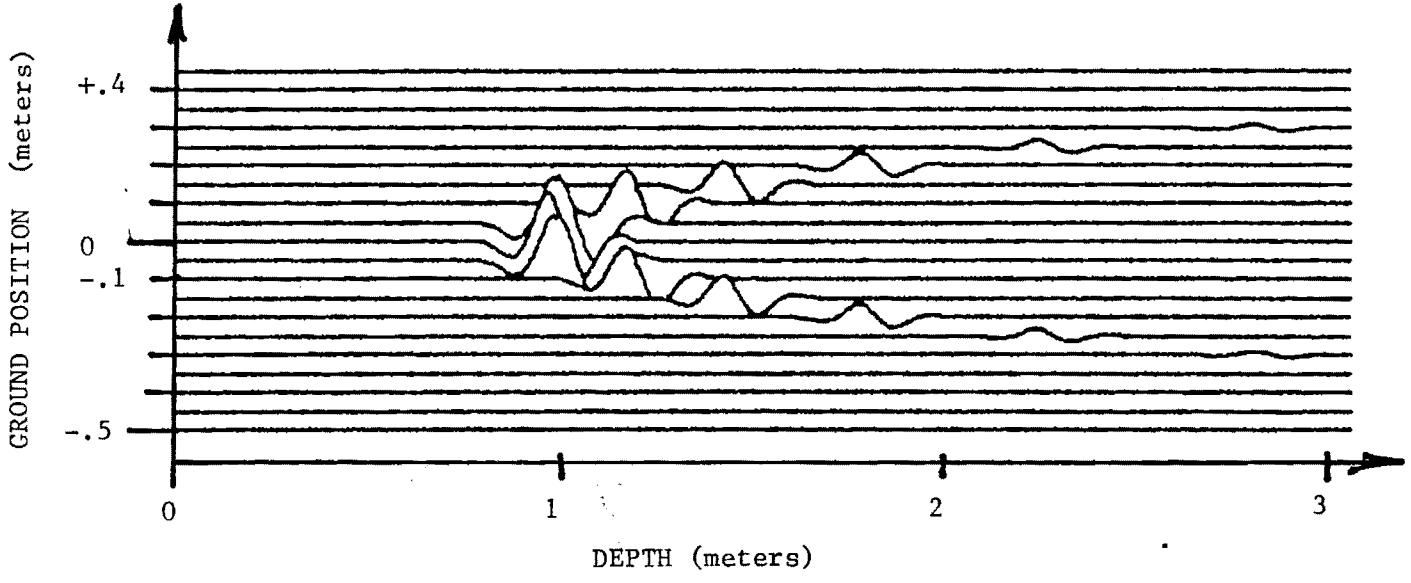

FIGURE 18 'PIPE' TARGET SIGNAL RETURNS

Beamwidth = 0.1 radians

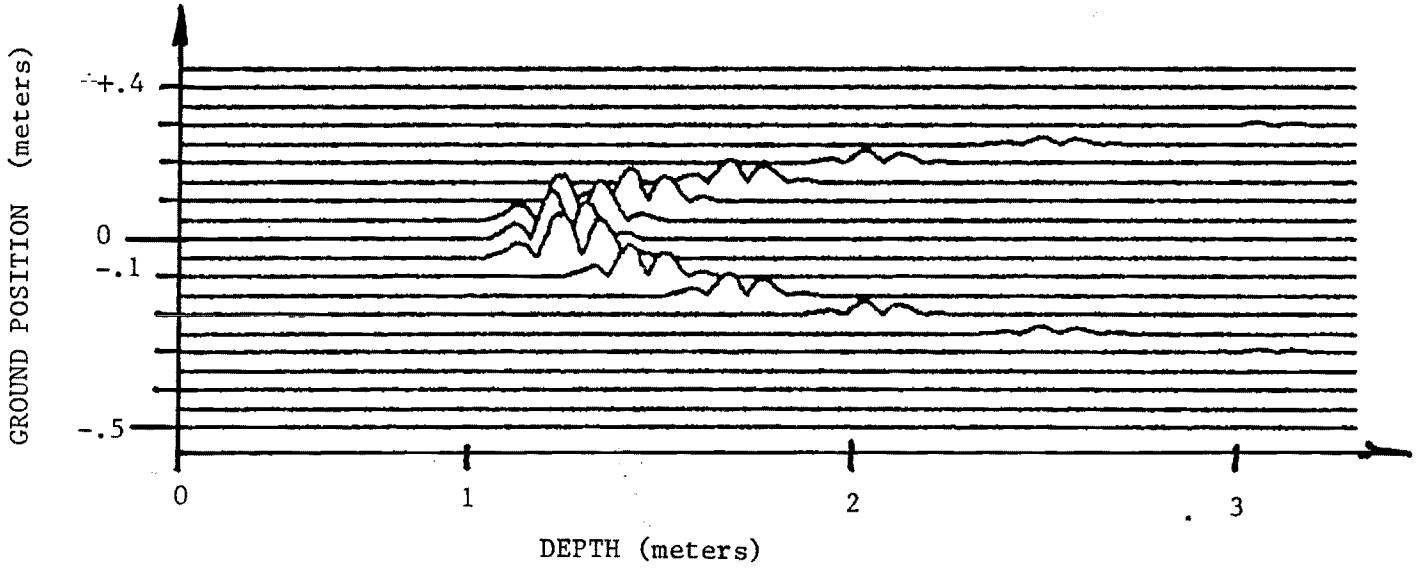

FIGURE 19 'PIPE' SIGNAL RETURNS - MAGNITUDE

beamwidth = 0.1 radians

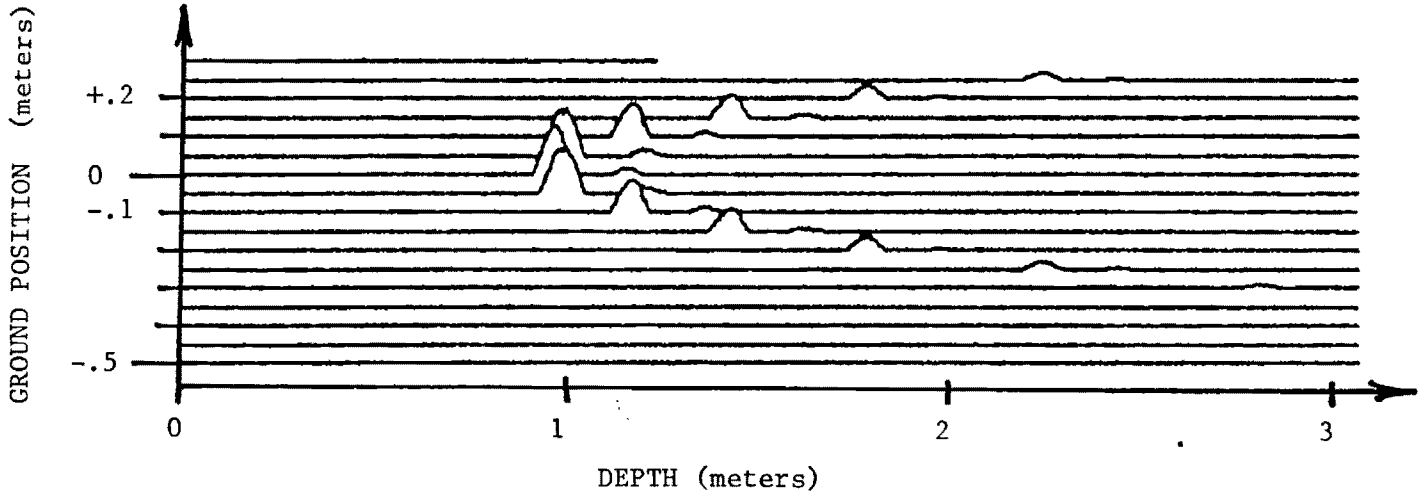

FIGURE 20 'PIPE' SIGNAL RETURNS - POSITIVE

beamwidth = 0.1 radians

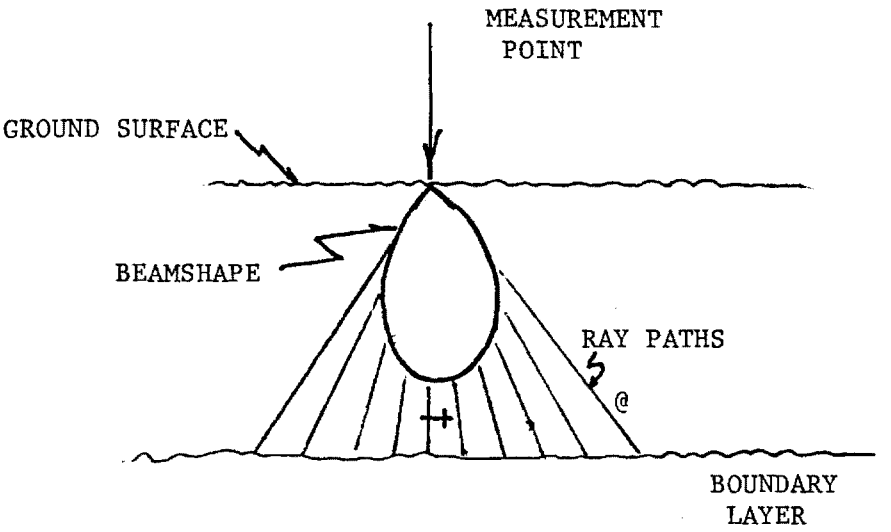

+ RAY PATH: minimum return signal delay
maximum reflection coefficient
maximum beamshape factor

@ RAY PATH: maximum return signal delay
minimum reflection coefficient
minimum beamshape factor

NOTE: Adding up signal returns from all angles lengthens the return signal pulse and 'spoils' the resolution.

FIGURE 21 PULSE LENGTHENING EFFECT

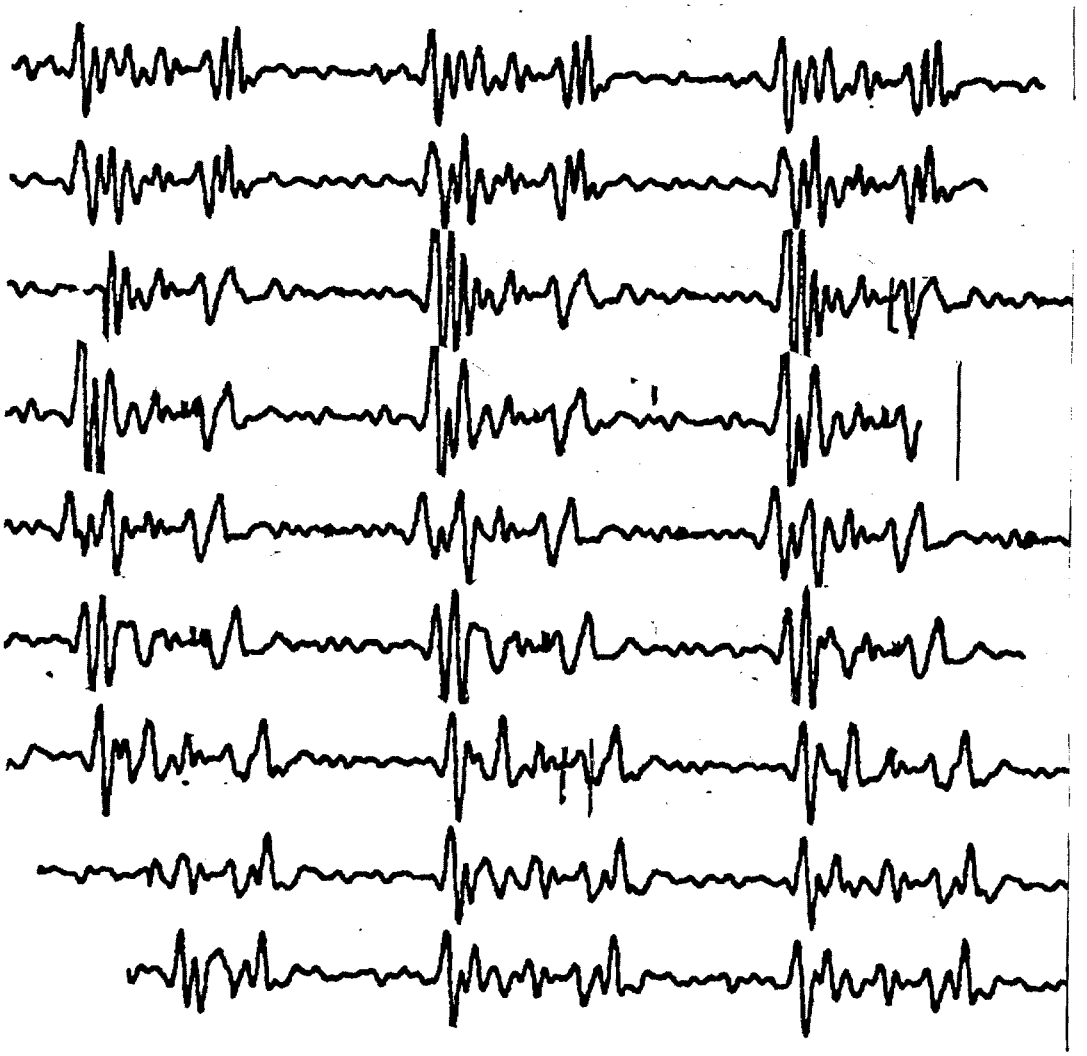

FIGURE 22 'SIR' SIGNAL RETURNS

(manually synchronized)

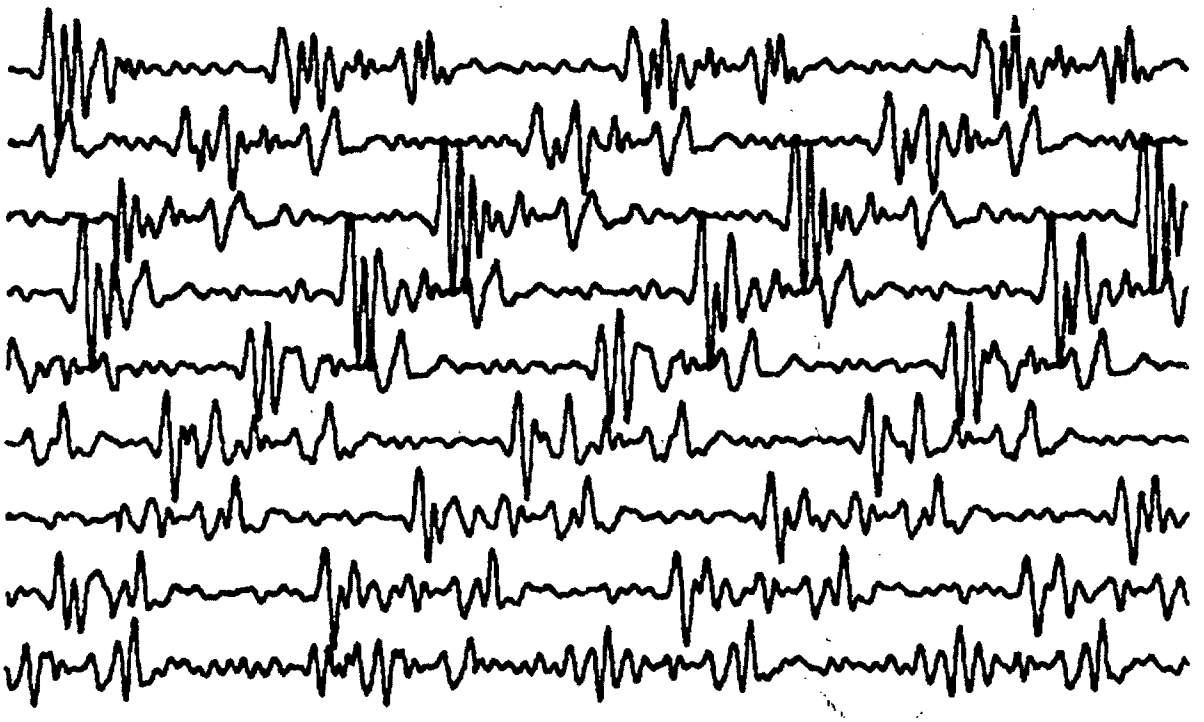

FIGURE 23 'SIR' SIGNAL RETURNS

(non-synchronized)

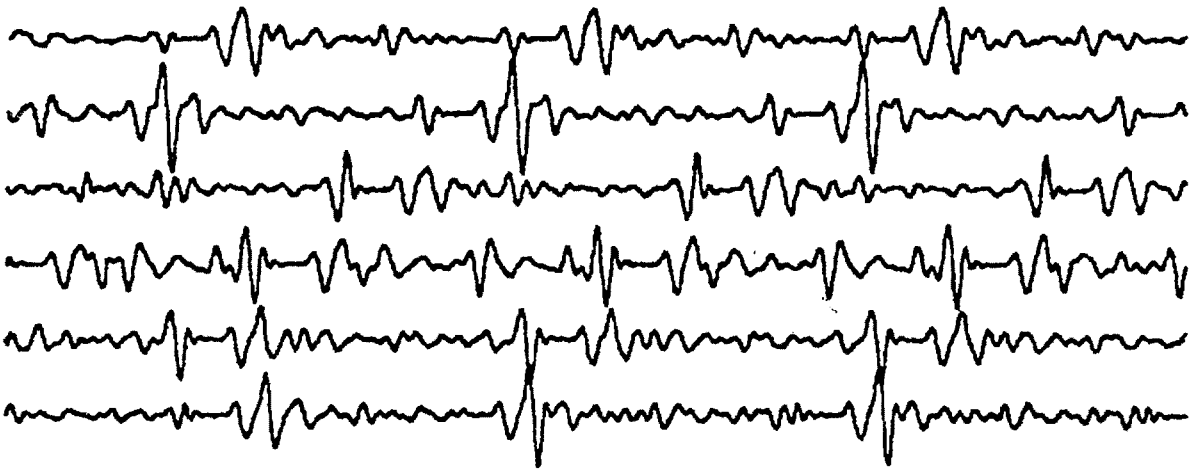

FIGURE 24 SELECTED 'SIR' SIGNAL RETURNS

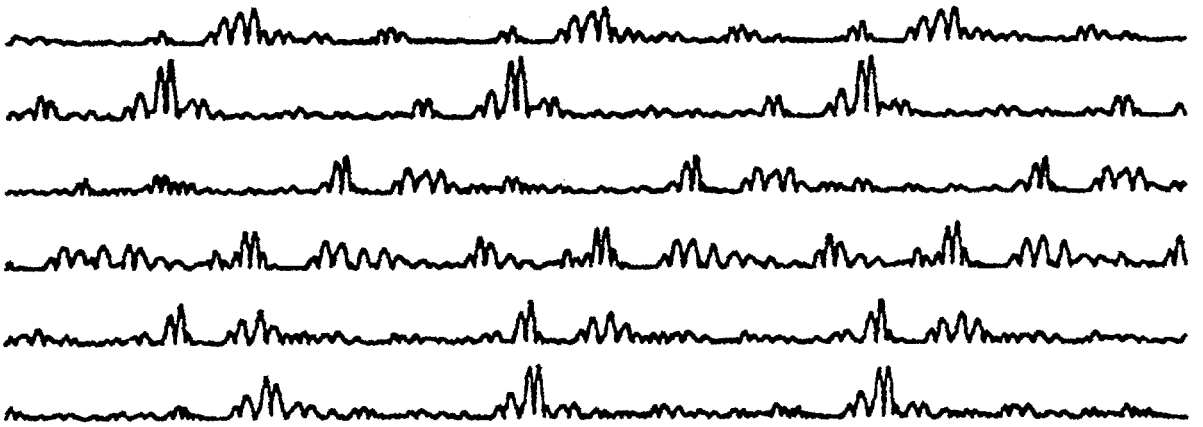

FIGURE 25 SELECTED 'SIR' SIGNAL RETURNS - MAGNITUDE

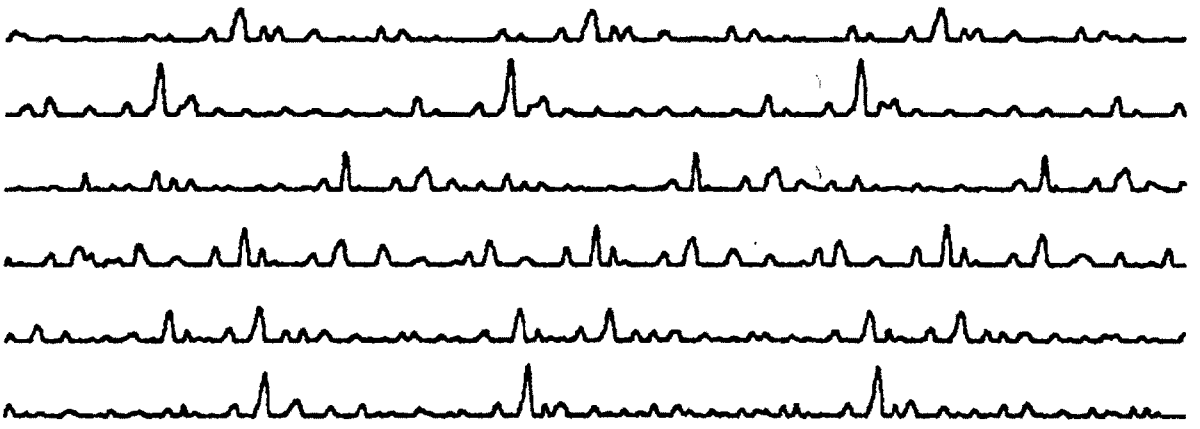

FIGURE 26 SELECTED 'SIR' SIGNAL RETURNS - POSITIVE

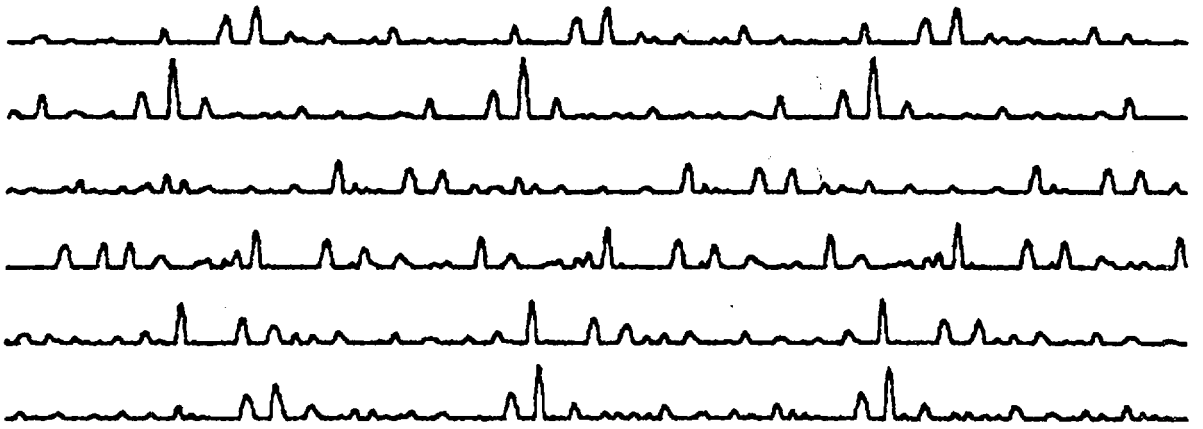

FIGURE 27 SELECTED 'SIR' SIGNAL RETURNS - NEGATIVE